6.4 Target and Target Fabrication

Target physics issues are not addressed in this section or in this report as all pertinent data have been supplied by the DOE Target Working Group (TWG).[1,2] Data on target gain and physics used in this report is also found in the TWG's recommended guidelines[1,2] and are summarized in Chapter 3. The question of illumination symmetry for direct drive targets may be considered a target physics issue and is discussed in Reference 1. However, the information supplied by the TWG pertains to beams with a $\sin^2 x/x^2$ profile. It will be much easier to supply beams with a somewhat different profile using the laser system proposed in this report (see Section 6.5). The question of illumination symmetry is, therefore, discussed in Section 6.4.1 to show that the proposed system will not lead to a deterioration in target performance over that prescribed in the TWG guidelines. Illumination symmetry is also used to examine the effect on target performance of various laser system malfunction scenarios.

The issue of target fabrication is addressed in Section 6.4.2. Alternative target fabrication techniques are reviewed and specific methods are chosen for this reactor design. Additionally, the question of target survivability is addressed in view of the various thermal, structural, and other stresses encountered by the target in the reactor system.

Section 6.4.3 is devoted to the target factory. It includes a discussion of the overall layout of the facility including the fabrication and inspection techniques employed therein. The section concludes with a discussion of target production costs and target factory staffing requirements.

The target injection system is covered in Section 6.4.4. Acceleration systems are proposed for both direct and indirect drive targets. Target tracking and beam steering systems are defined for both target types.

6.4.1 Target Performance - Data on illumination symmetry for direct drive targets was provided by the TWG for a 60-beam arrangement similar to the one described in Sections 6.3 and 6.8. As mentioned above, this information was obtained assuming a $\sin^2 x/x^2$ beam profile. However, it may be much easier and economical to generate beams with a flat, "top hat" profile with the laser system described in Section 6.5. The question of illumination symmetry for such beams has, therefore, been examined to insure that there is no unacceptable decline in performance from the data provided by the TWG.

6.4.1.1 Illumination Symmetry - Illumination symmetry and uniformity requirements on a direct-drive spherical target irradiated with multiple laser or other beams has been studied by a number of authors.[3-5] A formalism that has often been used to study uniformity of illumination is described in Reference 5. In this method, the

irradiation pattern on the sphere is broken down into spherical harmonics. Additional detail is added by using a single beam factor evaluated by tracing rays through the target plasma. A geometrical factor is also used to account for the number and orientation of the beams.

A view factor computer code was developed to study illumination symmetry for this reactor design study. The code uses algorithms common to similar codes developed to study radiation transport problems. However, the code has a number of unique capabilities not common to other view factor codes, such as the ability to model highly collimated beams arranged in arbitrary geometries and pointing in arbitrary directions. Although quite different from the formalism described in Reference 5, the code gave similar results on benchmark problems. The code breaks the target surface into some large number of elements of approximately equal area. It then uses information on the geometry and apodization of the illuminating beams to solve the geometric problem of where within the sheaf of each beam each of the target surface elements is intersected. This makes it possible to determine how much energy is received from each beam by each surface element. These quantities are summed for all the beams and the results are compared, allowing conclusions to be drawn regarding variations in illumination over the target surface. It is possible to introduce beam mispointing errors either manually or randomly, and to introduce energy imbalances between the beams. It is also possible to keep track of illumination symmetry as the target travels through space. At present, only surface illumination effects are modeled. The algorithm is flexible enough to allow for simulation of volumetric absorption effects should this become necessary. However, illumination symmetry results supplied by the TWG were closely duplicated without resorting to volumetric modeling. Unless otherwise noted, the results described in the following paragraphs apply to beams that have a top hat profile. The results were obtained for target surfaces subdivided into 500 surface elements. Greater surface resolution than this did not significantly change the results for the 60-beam system modeled. The beams were arranged as shown in Sections 6.3 and 6.8.

Figure 6.4.1-1 shows the effect on illumination symmetry of variations in the ratio of beam radius to target radius. This ratio is, of course, 1.0 for tangential focus. In an IFE reactor, the target would implode during illumination by a beam of uniform radius, causing the ratio to vary from 1.0 at the start to around 2.0 at the end of the laser pulse. For zoomed illumination systems, the ratio would stay at about 1.0 throughout the pulse. The curves in Figure 6.4.1-1 were generated assuming perfect beam energy balance with no mispointing. Under these ideal conditions, the top hat beam apodization results in a deterioration of illumination symmetry compared to the $\sin^2 x/x^2$ profile. The rapid drop off in performance seen for ratios less than 1.0 is especially pronounced for the flat profile. Clearly, illumination must be at least tangential for a flat apodization and, preferably, somewhat greater to allow for mispointing and beam jitter. The symmetry above a ratio of 1.0 is very flat, as

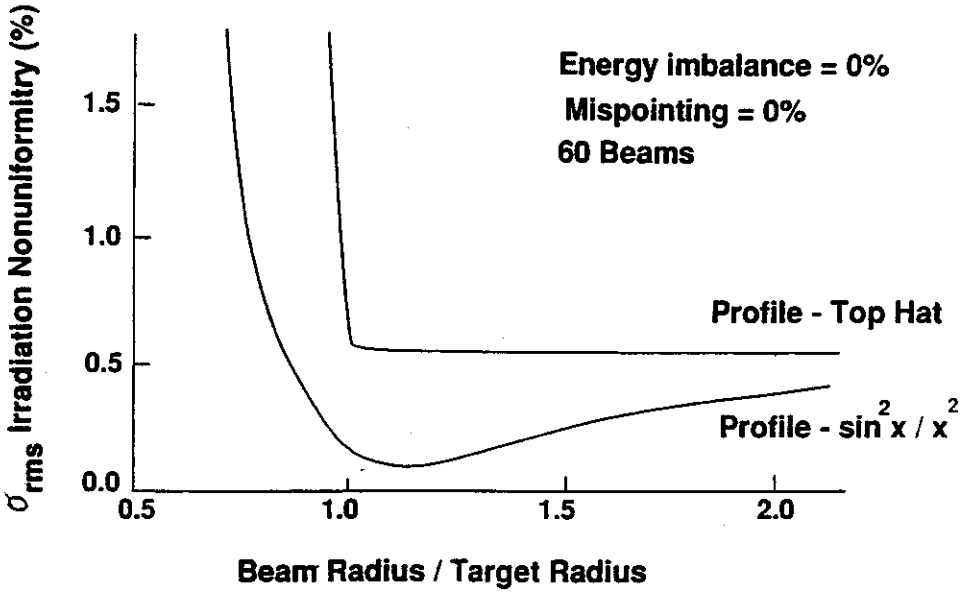

Figure 6.4.1-1. Beams with Top Hat Profiles Deliver Acceptable Illumination Symmetry

expected, since the intensity of the beam does not vary at any point in a cross section. For very large ratios, the $\sin^2 x/x^2$ profile begins to look flat to the target and begins to approach the top hat curve.

Evidently, under otherwise perfect conditions, some sacrifice in performance is made by going to flat beams. However, above a ratio of 1.0, the irradiation nonuniformity is still significantly below the target figure of 1.0 set by the TWG. It is, therefore, apparent that top hat beams can potentially meet reactor illumination symmetry requirements.

It is unlikely that the perfect beam pointing and energy balance conditions assumed above can actually be achieved in a working reactor. Figure 6.4.1-2 shows the effect on irradiation uniformity of random beam pointing errors. Beams were configured so that tangential illumination would have occurred in the absence of pointing errors. The curves in the figure were generated by choosing a maximum pointing error, and then mispointing each beam by a random fraction of this amount between 0.0 and 1.0. As these errors increase, the superiority of beams with the $\sin^2 x/x^2$ apodization becomes less marked and, eventually, disappears entirely. Interestingly, beam mispointing causes 60-beam systems with both apodizations to exceed the critical 1% root mean square irradiation nonuniformity level when the maximum mispointing exceeds about 0.07 of the target radius. This shows that beams with the top hat profile will not cause reactor performance to deteriorate faster than the $\sin^2 x/x^2$ apodization in the presence

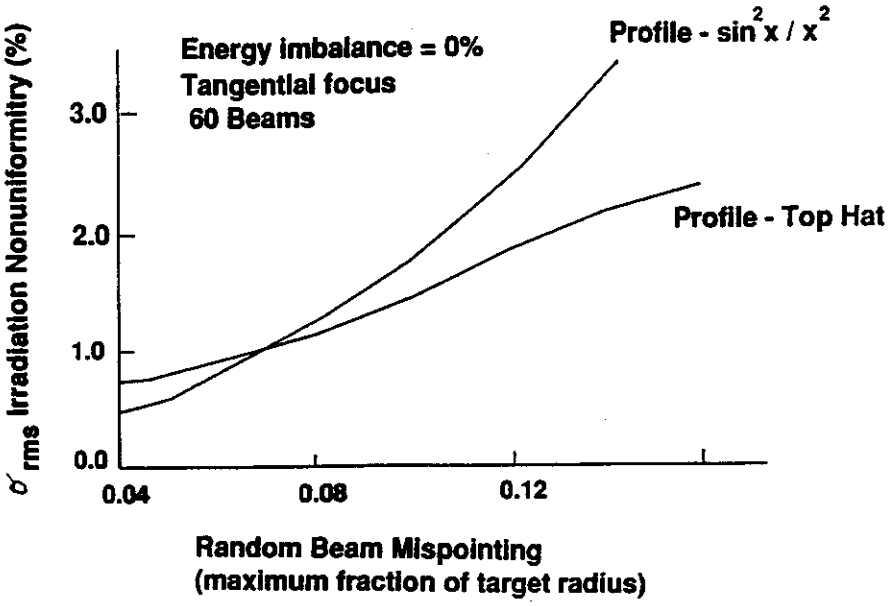

Figure 6.4.1-2. Top Hat Beam Performance Is Not Significantly Worse than that of Beams With $\sin^2 x/x^2$ Profiles in the Presence of Random Mispointing Errors

of small mispointing errors. In particular, the critical 1.0% illumination nonuniformity level will not be exceeded faster with top hat beams. This is significant because some mispointing error is probably unavoidable. It is noted that qualitatively similar curves to those shown in Figure 6.4.1-2 were obtained using different sets of random numbers. It was not, however, possible to conduct sufficient runs to determine statistically accurate error bars at all points.

The most likely laser system malfunction for the direct drive reactor proposed here would entail the loss of 1/16 of one beam, or 1/960 of overall laser energy. Results of such a malfunction are shown in Figure 6.4.1-3. The resulting illumination nonuniformity would not be significantly greater than that predicted under ideal conditions. Target performance would not suffer any significant decline. Also shown in Figure 6.4.1-3 is the result of the much more unlikely loss of one fourth of a single beam. Even under these conditions, the irradiation nonuniformity under otherwise ideal conditions does not exceed 1% for beam radius to target radius ratio greater than 1.0. Again, comparison with Figure 6.4.1-4 shows that performance of beams with the top hat profile is not significantly poorer than those with the $\sin^2 x/x^2$ apodization for loss of 1/4 beam. Calculations show that the loss of one entire beam out of the 60 would result in failure to properly implode the target for both apodizations.

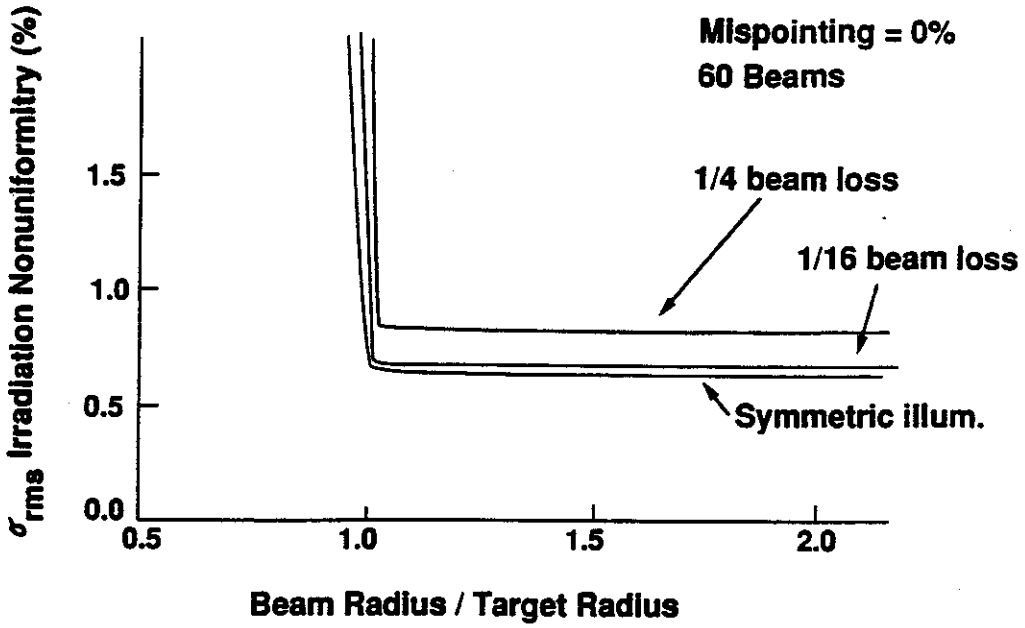

Figure 6.4.1-3. Reasonable Loss Scenarios Do Not Lead to Target Failure with Top Hat Beams

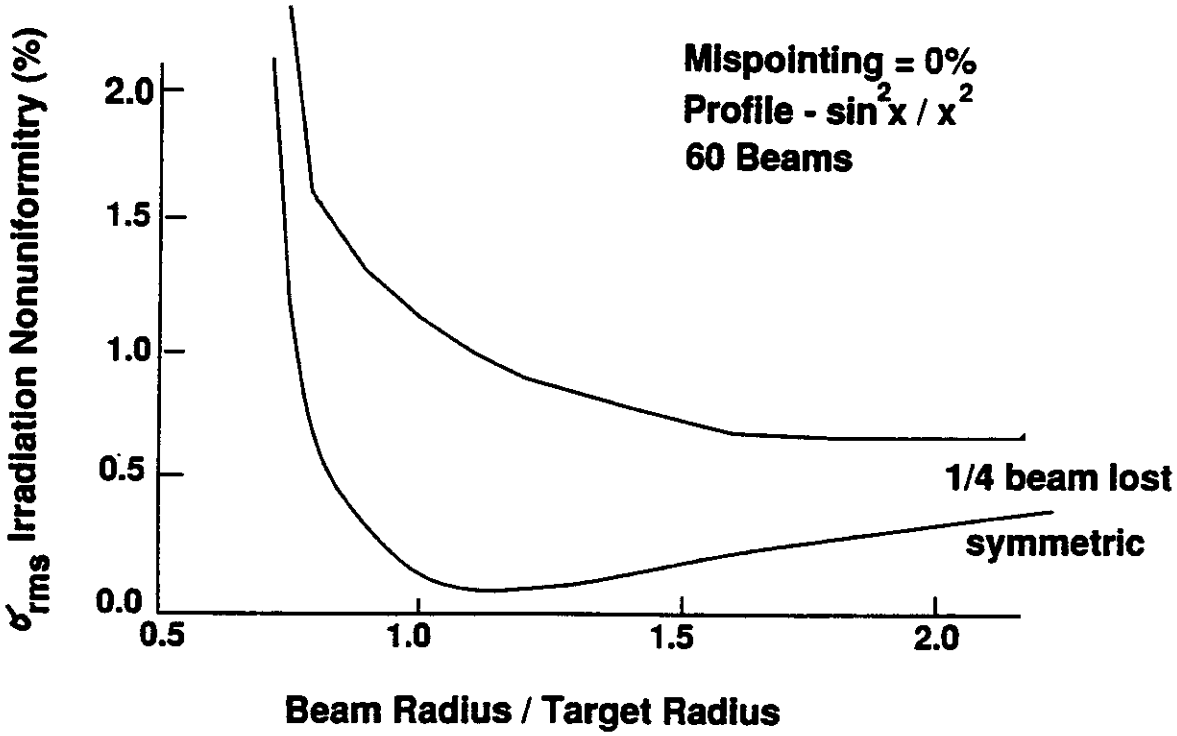

Figure 6.4.1-4. Beams With $\sin^2 x/x^2$ Profiles Do Not Show Significantly Better Performance in Beam Power Imbalance Scenarios

6.4.1.2 Target Heating in the Reactor Cavity - In the proposed direct drive reactor design, sabots will be used to protect the targets during acceleration in the injection system. However, the sabots will be separated from the targets before they enter the reactor cavity. The unprotected targets must reach the firing point before the cryogenic fuel layer is heated above the triple point by radiation and interaction with the gases in the cavity. Excessive target heating could force a reduction in the pulse repetition rate or redesign of targets with shine shields, ablative layers, or other protective schemes. Previous studies have raised serious concerns about the ability of unprotected targets to survive their journey through the cavity.[6] However, higher ambient cavity temperatures and/or pressures were assumed in many of the studies. For example, a cavity temperature of 2000°C was assumed in the Solase report.[6] We assume that cavity temperature will not exceed 600°C during target transit. Note that the target will not enter the cavity region until the cavity temperature and pressure are nearly at equilibrium conditions. Radiation tends to dominate the heat transfer to the target. Since radiation is proportional to the fourth power of the absolute temperature, serious problems at 2000°C do not imply that similar difficulties will exist at 600°C.

The target heating problem was examined with the aid of a 3D spectral method computer code. It was used to solve the non-linear heat equation,

$$\rho c_p \frac{\partial T}{\partial t} = \text{div} \left(k(T) \nabla T \right) + q$$

where:

- ρ = density in g/cm^3
- c_p = constant pressure heat capacity in joules/deg-g
- k = conductivity in watts/deg-cm
- q = volumetric heat source (non-zero only in DT ice)
- T = temperature in °K

and the boundary conditions were,

$$k_{shell} \frac{\partial T}{\partial n} = Q \text{ watts/cm}^2 \text{ (heat flux on shell surface).}$$

The code used Chebyshev polynomials and grid points in radius and spherical harmonic functions and grid points in latitude and longitude (spherical coordinates). A domain decomposition method was used making it possible for all parameters, such as k, c_p, q and r to vary discontinuously across material boundaries. Shell heat capacity was assumed constant at 1.754 joules/deg-g. The code can allow for temperature-dependent conductivities. However, since this dependence is not well understood at very low temperatures, shell conductivity was also assumed constant for each run. A range of plausible conductivities were then checked in separate runs.

Target temperature distributions were checked after 0.1 seconds, a maximum assumed transit time of targets through the cavity. (Note that the final design for the direct drive injection scheme reduces the target transit time to 0.0375 seconds for a velocity of 200 m/s over a distance of 7.5 m. This conservative estimate will compensate for time to accelerate capsule and transit through the shielded blanket region.) The target examined was that prescribed by the target working group scaled to a driver energy of 4 MJ. An ambient pressure of 3 mtorr was assumed for the direct drive (DD) targets. A sample of the results obtained with the code is shown in Table 6.4.1-1.

Table 6.4.1-1 Effects of Cavity Environment on Direct Drive Targets After 0.099 sec. (3.0 mtorr H)

Ambient Temp, K	Shell Thermal Conductivity, W/K/cm	Ice/Vapor Temp, K	Ice/Shell Temp, K	Outer Shell Temp, K
2000	1.0×10^{-3}	11.17	11.87	776.30*
700	2.0×10^{-3}	10.23	10.30	18.20
800	2.0×10^{-3}	10.39	10.50	24.00
1000	2.0×10^{-3}	10.91	11.21	4.18
2000	2.0×10^{-3}	19.68	29.62*	556.90*
700	4.0×10^{-3}	10.80	10.95	15.89
1000	4.0×10^{-3}	13.03	13.96	34.53
700	8.0×10^{-3}	11.45	11.68	14.36
1000	8.0×10^{-3}	15.40	16.99	28.17

* Shell outer surface temperature above CH damage threshold and/or DT ice temperature exceeds the triple point.

Table 6.4.1-1 shows that, at 3.0 mtorr, much higher temperatures than those expected in the reactor design presented here for DD targets would be necessary to cause significant target damage or deterioration, even in the unlikely case that the target absorbed all the radiative energy impinging on its outer surface. No shine shield or other special precautions would be necessary to avoid target thermal damage in the reactor cavity. Should the expected DD reactor cavity temperature and pressure during target injection prove unrealistically low, it would still be possible to overcome target heating problems by increasing injection velocity, thereby decreasing the amount of time the target is exposed to the cavity environment. According to the data presented in Reference 7, the DD targets should survive accelerations much higher than those required by the design presented here.

Ambient pressures in the indirect drive reactor cavity during target injection are expected to be similar to those for direct drive. Since ID heavy ion targets are completely enclosed in a radiation case, they are inherently more resistant to problems with overheating than their direct drive counterparts. A simple analysis of heat conduction in such targets shows that, even at pressures of 100 mtorr, no DT ice

melting will occur after 0.1 seconds. In other words, at design temperatures, indirect drive targets should be able to survive ambient pressures more than an order of magnitude higher than expected within the target cavity. Furthermore, at the 500 K to 600 K cavity ambient temperatures expected in the indirect drive reactor system proposed here, no significant damage to the radiation case material should occur.

6.4.2 Target Fabrication - In this section fabrication methods for the major components of direct and indirect drive targets are discussed. Many of the techniques described have actually been used to produce targets for IFE experiments. Unfortunately, none of them has succeeded in demonstrating a capability to mass produce reactor size targets. In large part, this probably results from the lack of an immediate need for a large quantity of reactor size targets and the consequent lack of R&D funds devoted to their development. It should be straightforward, for example, to fabricate radiation cases for indirect drive targets and sabots for direct drive using existing technology. In spite of the many promising fabrication techniques described below, however, the same cannot be said of target shells. Reactor size shells can certainly be made using very expensive microfabrication and micromachining techniques. However, fabrication of such shells has not yet been demonstrated using droplet generators, microencapsulation, and other promising techniques for economical mass production. In the following section the case is made that this should not necessarily disqualify these techniques from consideration as candidates for reactor target mass production.

6.4.2.1 Target Shell Fabrication - Numerous techniques have been tried for producing target shells for experimental IFE facilities. A number of these show promise as methods for mass producing targets for IFE reactors. Some of the techniques are reviewed below. The methods described do not represent an exhaustive list. For that matter, it is quite possible that none of them will be chosen to produce targets for future reactors. A glance at "The Journal of Vacuum Science and Technology," or a similar publication in the field of applied chemistry is enough to impress one with the huge number of techniques that may someday have an impact in controlled fusion. Significant research and development resources have not yet been committed to developing ways of mass producing reactor size plastic target shells. When they are, it is not unlikely that new techniques will be developed which will supersede all the processes described here. The goal of this section is not to prescribe what the eventual shell fabrication technology will be. Rather, it is to make the case that, if necessary, reactor-size targets could be economically mass produced, if not with off-the-shelf technologies, at least with modest extensions thereof.

Historically, the vast majority of experimental laser fusion target shells have been composed of glasses of various types. Such shells can be produced by injecting drops of aqueous solutions of the glasses into the top of a drop tower or vertical tube furnace. Glass shells are formed as the drops fall through the furnace and are

collected at the bottom. This technique offers excellent control over shell mass and size. However, it is limited to a relatively narrow range of compositions and production of relatively small shells.[8] In a somewhat similar but more versatile technique, the components of the glass are placed in solution and converted into a gel. This material is crushed into a fine powder. A sieving step separates the powder into particles of the desired size. The material is then introduced at the top of the drop tower. It is possible to produce plastic shells using variations of the above techniques. However, it will probably be impossible to produce simple blown shells at the size and thickness levels necessary for IFE reactors.[9] Fortunately, promising alternatives to the procedures outlined above have been demonstrated. Some of these are described below.

Droplet Generators/Microencapsulation - In the various versions of microencapsulation, polymer layers are formed around droplets of volatile liquid in a suspending medium. The liquid is then removed by evaporation or some other exchange procedure leaving behind a plastic shell. In one version of the process,[10] an aqueous phase is emulsified in an organic solution of the desired polymer; subsequently, the oil/water emulsion is poured into a second water phase yielding a water/oil/water emulsion. The solvent is driven off thermally, leaving polymer shells containing water. The water is removed by gently heating the shells in vacuum. This procedure has been used to make CH shells. In an adaptation of the same process, CH shells with PVA permeation barriers have been produced. In the method described above, droplets are formed by rapid stirring of the mixture. This allows for little control over droplet size and thickness. To alleviate this problem, droplet generators with double and even triple nozzles have been introduced. These make it possible to exert much greater control over shell geometries. Shells can be produced from the droplets by allowing them to fall through heating towers or introducing them into a microencapsulation medium.

It presently appears unlikely that blown shells with diameters greater than about 1 mm can be produced within the tolerances demanded for inertial fusion targets. Droplet generators combined with microencapsulation are a promising alternative. Targets of the size and thickness needed for future IFE reactors have not yet been created using these techniques. However, there has, yet been no great demand for them. There is much room for progress in this field if significant research and development funds are made available. This seems justified considering the adaptability of these processes to the demands of mass production and their ability to produce uniform, seamless shells with excellent surface characteristics.

Micromachining - Several micromachining techniques have been used with good success to produce targets larger than those generally available from such processes as microencapsulation and drop tower blowing.[11,12,13] The term micromachining will be used to refer to a number of techniques that have been applied for fusion target

fabrication, including, among others, single point diamond turning, diamond sawing, laser drilling, and mechanical polishing. A significant application is in the creation of hemispheres that can be mated to form target shells.

The application of single point diamond turning to production of IFE targets was pioneered at Los Alamos and Livermore National Laboratories.[14,15] The technology existed before the need for fusion targets arose. However, the delicate nature of the work involved made it necessary to refine control of temperature, vibration, etc., on existing devices. Reported applications have included machining of support stalks from mandrels used to facilitate plastic coating of glass spheres. Extremely smooth surface finishes can be achieved in this way. It may be possible to apply a similar technique in future target factories as a final finishing technique for shell surfaces. Single point diamond turning has also been used to create hemispherical shells. In one technique, a convex mandrel was first machined. A layer of coating material was then deposited over the mandrel, and excess material was machined away. The mandrel was then dissolved to leave a hemispherical shell. Variations of this process have been used to produce shells with a step across the edge to facilitate mating. Stringent tolerances and surface finishes are necessary to successfully mate hemispheres for fusion target applications. This is a serious objection to the use of hemisphere mating for target mass production. Single point machining is one way of meeting the required tolerances. However, control of large numbers of such lathes in a future factory would be a daunting task.

Laser cutting has also been used to produce hemispherical sections by rotating the surface of a hollow shell through the focal point of the laser beam. However, the finite cut width of the laser beam makes it very difficult to produce hemispheres that can be accurately remated in this way.

Laser drills have been used to create tiny holes in target shells, which can then be used to introduce high-Z gases for use as diagnostics. A similar technique could be used in a target factory as part of a drill and fill operation should the tritium inventories and fill times required by the diffusion filling process prove excessive.

The so-called void formation method, which has been used to create large glass and plastic shells,[16] employs several micromachining techniques. The process consists of forming a spherical bubble in molten material, then grinding away the excess material to form a shell. The material can be rotated during the process to minimize the effect of bubble movement. In an application of this technique reported in the literature, the molten material solidified into a cylindrical mass after void formation. A diamond cutting wheel was used to cut a rough cube containing the bubble from this mass. Diamond saws were then used to form a rough sphere. The capsule is then placed in a lapping system consisting of three lapping mandrels, as shown in Figure 6.4.2-1, which is capable of grinding and polishing the surface to any desired thickness.

Large, seamless, uniform shells can be created in this way. Unfortunately, the process is extremely labor intensive, and is an unlikely candidate for mass production of targets.

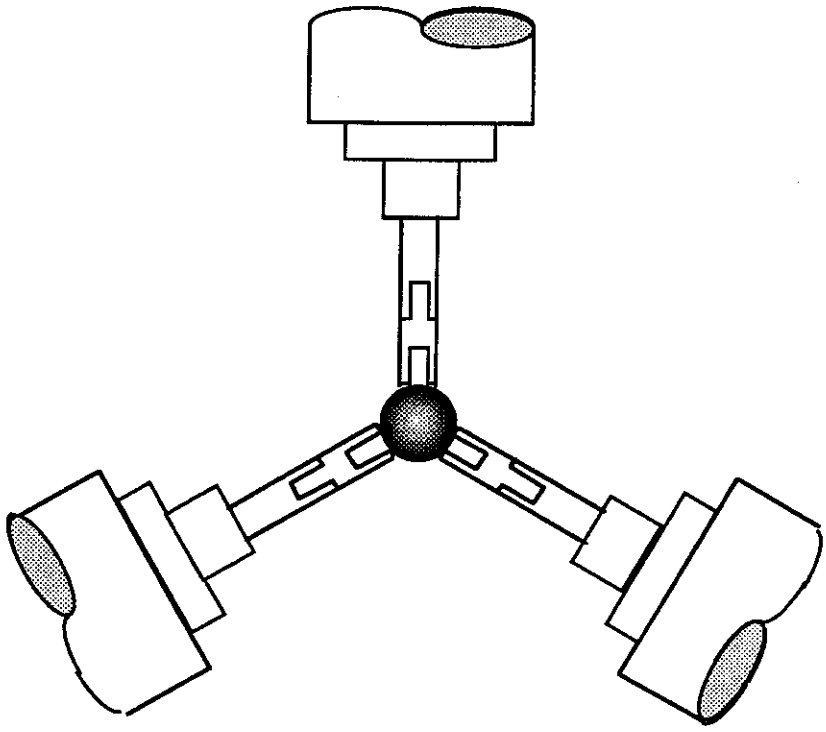

Figure 6.4.2-1. Shell Held in Place by Three Laps, Driven by Independently Controlled Motors

Hemisphere Fabrication and Joining - Hemispheres can easily be filled with fuel and then joined together to form target shells. Lengthy diffusion filling steps requiring large tritium inventories can be avoided in this way. Unfortunately, it may be difficult to produce the hemispheres with sufficient precision for fusion target applications and keep their costs within reasonable bounds at the same time. Micromachining techniques for producing hemispheres have already been described above. Other methods which are more promising for eventual mass production include chemical etching and solid-state processes.[17,18]

One such technique takes advantage of the relatively advanced state of development of glass shells for fusion applications. Such shells are sputter coated with a copper release layer and then embedded in epoxy. The epoxy is then reactive ion etched in oxygen down to the equator of the glass shell. When the shell is removed from the epoxy, a negative hemispherical mold is left behind in the epoxy surface. This surface is replicated using a silicone rubber compound. The positive rubber replica is used as a master mold for making any number of final molds. This is done by curing a drop of photoresist on the rubber master mold. Once a metal substrate is epoxied over the top of the photoresist and allowed to cure, the silicone master can be peeled away for

eventual reuse, leaving the photoresist final mold mounted on the metal substrate. These molds can then be coated with any chosen shell material. Hemispherical shells with excellent surface quality have been produced using this method. Unfortunately, the size of the high quality blown glass shells used in the process is presently limited to about 1 mm. Production of thick shells with fine edge tolerances is also difficult using the method.

A method that shows more promise for producing large, thick, hemispherical shells borrows techniques developed in the semiconductor industry. The mass production of silicon computer chips provides ample evidence of the utility of such techniques in producing large numbers of identical objects.

In the basic process, hemispherical cavities are first formed in silicon wafers using batch photolithography and isotropic etching. Techniques exist for creating self-aligned flanges on the edges of these cavities. Once a hemispherical cavity is formed, its surface can be doped with a material that renders it insoluble to silicon etchant. The remainder of the wafer can then be etched away leaving a hemispherical shell. Alternatively, the hemispherical cavities can be used as molds for other material. To create thick shells, the entire cavity can be back filled with a selected material, which is then polished down to the level of the original masking layer on the surface of the silicon wafer. A hemispherical cavity is then formed in this material using the same photolithographic pattern definition and isotropic etching techniques used to create the original hemispheres. The finished hemispherical shell can then be freed from the surrounding wafer. Large, thick shells with excellent surface finish can be made in this way.

Target Shell Fabrication for the Prometheus Reactors - Droplet generators combined with microencapsulation have been chosen as the target shell fabrication technique for the Prometheus reactors. As already pointed out above, shells of the size and thickness necessary for future reactors have not yet been demonstrated using these processes. However, this reflects the lack of research and development devoted to production of reactor-size targets more than the unsuitability of droplet generators and microencapsulation for producing them. The very fact that there is so much potential for progress in this area is a good reason for not overdesigning shell fabrication facilities at this point. Even in the unlikely event that no further progress is made in these technologies, ancillary technologies in combination with some of the other techniques described above could be used, taking shells produced by droplet generators/microencapsulation as a starting point, to produce shells suitable for fusion reactors. Glow discharge polymerization (GDP), for example, has been used to fabricate CH coatings on fuel shells. It could be used to increase the thickness of polymer shells. It produces hard, strong, tough surfaces and good adhesion to existing surfaces has been demonstrated.[19] Significant technological progress has been made recently in achieving smooth surface finishes using GDP. Other promising

coating technologies exist which, alone or in combination with micromachining steps for grinding away excess material, could be used to increase the thickness of shells as necessary.

For purposes of designing the overall target fabrication facility a shell production procedure similar to that shown in Figure 6.4.2-2 is assumed. Provision for extra coating steps and generation of droplets with multiple layers is not shown in the figure. This does not reflect the belief that no such procedures will be necessary, but that it is impossible to predict their exact nature at this point.

6.4.2.2 Fuel Filling Procedure - Diffusion filling has been chosen as the fueling method for this design. It relies on the extremely high permeability of CH shells to hydrogen to allow filling within reasonable times. The fueling process will begin with a preheat step to drive residual gases out of the target shells. The preheat step will have dual benefit of degassing shells and making them stronger at the same time. The goal will be to constantly maintain optimum filling rates during the entire process while avoiding damage to the shells due to excess pressure.

The diffusion filling process would take place in a pressure vessel such as that shown in Figure 6.4.2-3. Empty shells received from the shell fabrication area would be introduced into the low pressure end of such vessels through a pressure lock. A number of the pressure vessels, perhaps as many as ten to fifteen, could be arranged in parallel. This would allow for periodic maintenance or replacement of individual vessels and an excess filling capacity should this be necessary, for example, to provide targets to other facilities, or to store targets on site for immediate restart after

short reactor shutdowns. Once loaded into the diffusion filling vessels, targets would be automatically conveyed through a number of zones of gradually increasing pressure separated by pressure locks. Maximum fill pressures would be about 800 to 1200 atmospheres. A heating system would maintain temperatures in the vessels at constant levels. A temperature of approximately 200°C would be optimum for rapid target fill, but it may be necessary to limit actual temperatures in the vessels to around 100°C to avoid softening damage to the polystyrene shells as well as excess leakage of tritium through the vessel walls and deterioration due to hydrogen corrosion and embrittlement. A limited amount of breakage of faulty target shells could be expected under the extreme conditions in the pressure vessels. However, experience with diffusion filling of the much more fragile experimental targets now in use has shown that neighboring shells seldom suffer significant surface or other damage when this happens. Fill times will depend on the exact thickness and state of polymerization of the plastic shells. However, assuming permeabilities near those of the experimental CH shells produced to date, fill times will likely be about 24 to 36 hours. The larger of these numbers is used in estimating required tritium inventories.

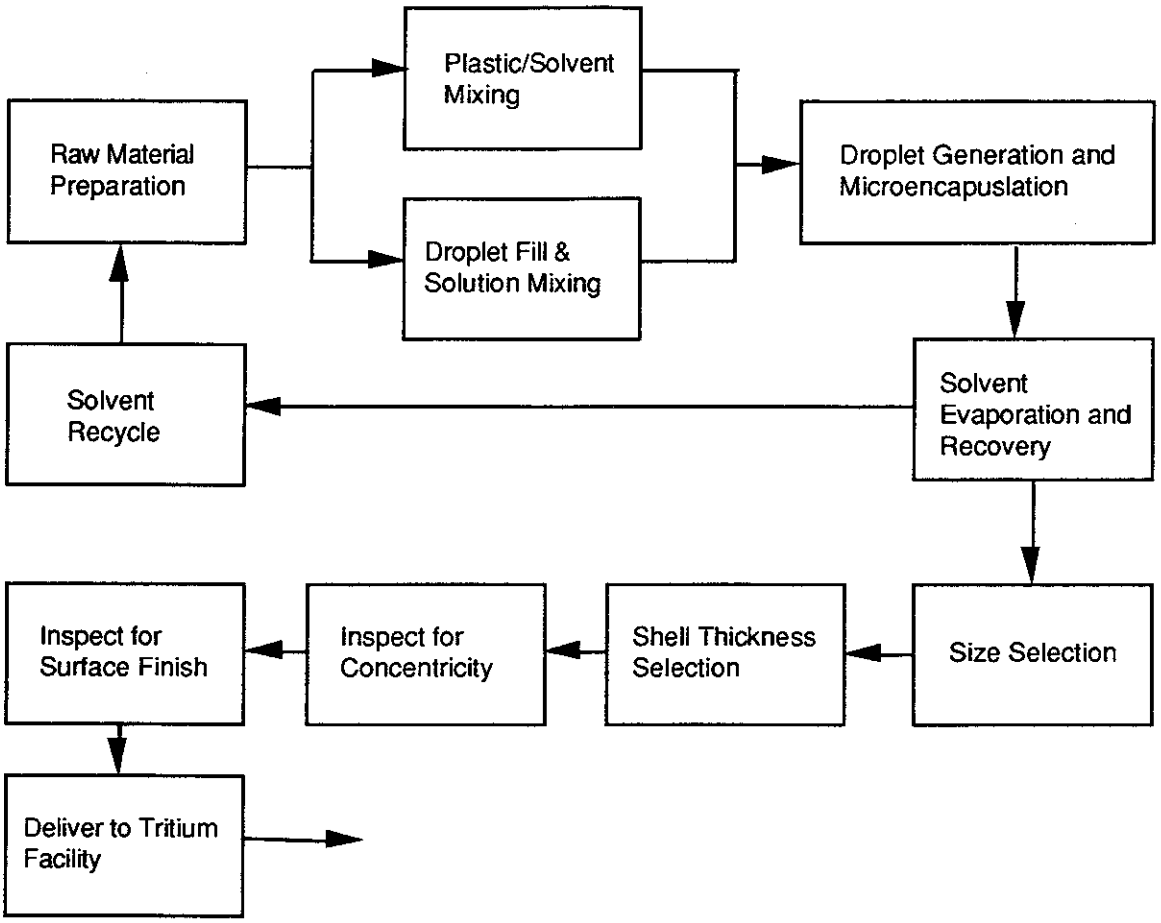

Figure 6.4.2-2. Target Costs Can Be Kept Low if Present Shell Production Technologies Can Be Enhanced to Produce Reactor-Sized Targets

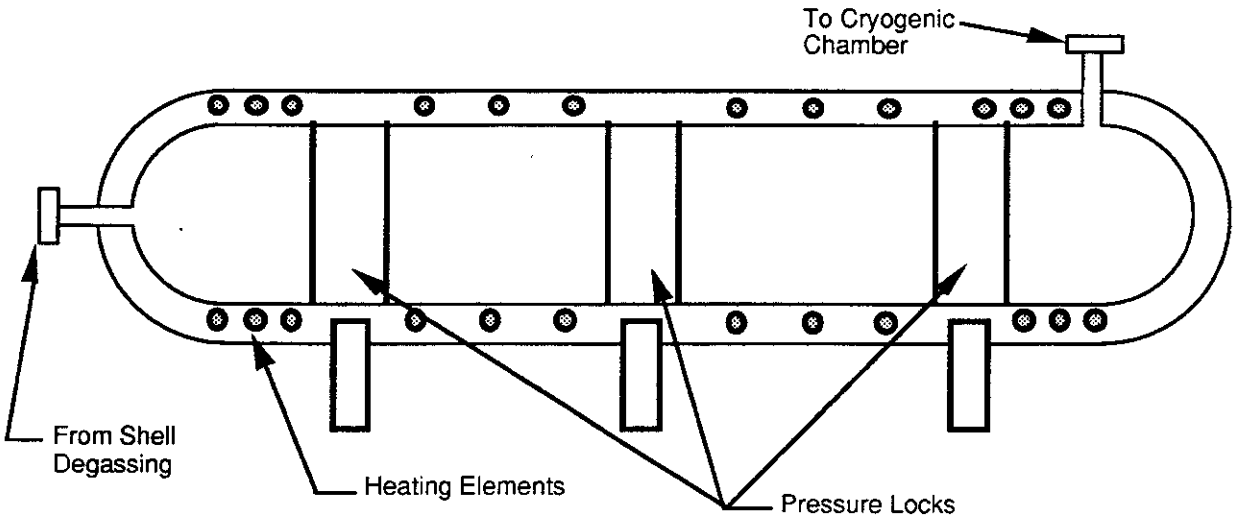

Figure 6.4.2-3. Pressure Vessel for Diffusion Filling

Hydrogen attack and hydrogen embrittlement of the pressure vessels could pose severe problems if conventional steel vessels are used in the diffusion filling process. In hydrogen attack, methane forms internally, causing the steel to swell and lose strength, eventually resulting in material failure. This mode of failure is uncommon at temperatures less than 200°C, but may become a problem at the extremely high pressures necessary for diffusion filling.[20] Hydrogen embrittlement refers to a complex of physical processes that are still not thoroughly understood. However, its effects can be devastating at much lower pressures and temperatures, leading to reduced fatigue life, surface blistering, internal fissuring, and reduced stress rupture.[21] Certain varieties of austenitic stainless steels have shown good resistance to hydrogen damage. However, even they are not immune.[22] The best solution to this problem would seem to be the use of aluminum pressure vessels. Aluminum and related alloys seem to be practically unaffected by hydrogen damage, even at high pressures. This characteristic is not dependent on the formation of an oxide layer, and is true of weldments as well as the base metal.[23] Some deterioration in the ability of aluminum to resist hydrogen damage is seen when hydrogen at high temperatures and pressures is combined with a high relative humidity. However, such problems should not arise as long as care is taken to control humidity.

Tritium inventories required in a factory depending on the diffusion filling process may be higher than those in facilities relying on some competing processes. However, they need not be excessive. The density of solid DT is 0.213 g/cm^3. The target would have a layer of this material about 600 microns thick if scaled to a driver energy of 5 MJ. The total DT mass would be about 7.5 mg. To provide such a mass, the entire interior of the target must be filled with DT gas at a pressure of approximately 600 atmospheres. This means that, in the final stage of the filling process, it would be necessary to surround the target with DT gas at a considerably greater pressure to assure a rapid fill. In the early stages of filling, outside gas pressure would be considerably less if the stepwise filling process outlined above is used. One can assume an average fill pressure for the entire process of around 500 atm, corresponding to a gas density of around 0.1 g/cm^3 at a fill temperature of 100°C. The CH shells must be surrounded by this pressurized DT during the entire diffusion filling step, which will take approximately 36 hours. Close packed spheres have a packing fraction of 0.74. The figure for randomly packed spheres is usually given as somewhere at the high end of the 0.5 to 0.6 range. Allowing a reasonable amount of space for automatic conveyor mechanisms, pressure locks, etc., one can conservatively choose a packing fraction of 0.5.

For a repetition rate of 4 Hertz, around 350,000 targets will be consumed per day. This implies that 525,000 targets will be in the diffusion filling stage if the fill time is 36 hours. Assuming the targets have a radius of 3 mm, each will occupy a volume of around 0.11 cm^3, and enclose a space of around 0.08 cm^3. For the 0.5 packing fraction cited above, 525,000 targets must then be surrounded by approximately

60,000 cm^3 of DT at 500 atmospheres. This gas will have a total mass about 6.5 kg, corresponding to about 4.0 kg of tritium. The average fill pressure in the targets during the process will be about 250 atmospheres. The 525,000 targets will, therefore, contain about 0.003 grams of additional DT each on average during the fill, accounting for another 0.95 kg of tritium.

If the beta heating process described below takes another four hours, another 87,500 targets will be in this stage of production at any time, corresponding to another 0.40 kg of tritium.

The total tritium required in the beta heating and diffusion filling stages alone, then, is around 5.35 kg. Inventory in piping, stored targets, compressors, etc., will likely bring the total inventory in the factory to around 7.0 kg. This corresponds to an activity of 6.8×10^7 curies. Thus, the diffusion filling process requires a rather high tritium inventory. However, it will require none of the potentially expensive and technically difficult mechanical processes described above, such as drilling, plugging, gluing, molding, etc. It will not be necessary to provide for the individual fueling of each of several hundred thousand targets per day. Human intervention in the filling process could be kept to a minimum, making it possible to keep personnel requirements in the tritium fill section of the factory low, thus enhancing the overall safety of the plant. Furthermore, diffusion filling makes it possible to avoid surface seams, cracks, holes and other imperfections occurring at mechanically joined or drilled surfaces that could potentially cause degradation in target performance, perturbation of the beta heating process and target disintegration under high acceleration.

A possible drawback to diffusion filling is potential tritium irradiation damage to the CH shells during the relatively long fill times. Significant damage to inner layers could occur in less than 100 hours.[24, 25] This can be a problem in small, experimental targets, where such damage can lead to shell failure. It is most unlikely that tritium irradiation will lead to such problems in reactor-size targets with their much thicker shells.

6.4.2.3 Creation of Uniform Fuel Layers - Excellent results have been achieving with the fast-refreeze method in creating uniform fuel layers for targets with diameters up to a millimeter and fuel layers of a few microns.[26] However, for the shells with radii of several millimeters and proportionally thick fuel layers, this method is not successful.[27] Use of low-Z foams as wicks for liquid DT has also been proposed as a way of creating uniform layers. Unfortunately, foam targets would have significantly lower gain than ones of similar size with free-standing ice layers. (TWG communication)

The beta heating method is proposed for creating uniform DT ice layers. This method relies on several simple physical phenomena to create uniform DT ice layers in spherical targets.[28] The relatively low energy beta released in the decay of the

radioactive tritium component of the DT ice is absorbed close to its emission point within the ice layer. This leads immediately to the generation of thermal gradients in nonuniform layers. The DT layer within a plastic shell can be modeled as a closed, solid-vapor system. In such a system, temperature gradients must be released by sublimation. In thick regions of ice, relatively more energy will be released because of the greater number of decaying tritium atoms. This will cause the thick regions to become warmer and the ice in such regions to sublime faster. In the thin regions the opposite is the case. Sublimation is slower and ice redeposition is faster. This process will continue in a spherically symmetric system until the ice layer is uniform as shown in Figure 6.4.2-4. The beta heating process could be used in conjunction with other, simpler techniques to increase the speed of the overall redistribution process. Air tumbling, for example, might be used during initial freezing of the ice to produce approximately even layers. This would shorten the time necessary for the beta heating process to create targets with ice layers sufficiently uniform to achieve high gain. Feasibility of this preliminary tumbling step would depend on such factors as potential damage to surface finish. Application of external thermal gradients could also be used as a preliminary step to generate nearly uniform ice layers.[29] Whether such preliminary steps will be needed depends, of course, on the ice redistribution rates in the beta heating process itself. Recent computer and experimental results seem to indicate that they can be eliminated.[30,31]

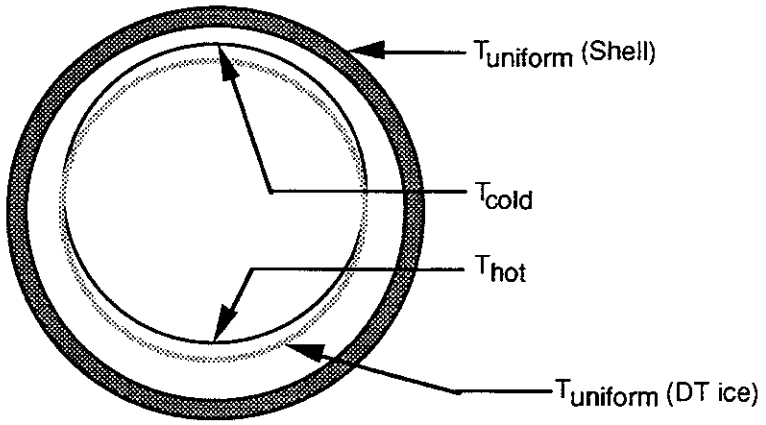

Figure 6.4.2-4. Energy From Beta Decay Can Form a Uniform Solid Layer of DT Fuel

The question remains of whether the process would be fast enough for mass production in an IFE reactor target factory. Fast ice redistribution to form uniform layers would be necessary to avoid deterioration of targets due to radiation damage and to eliminate the need for excessive tritium inventories. Recent theoretical and experimental work indicates that ice layers with sufficient uniformity for reactor targets can be achieved in a matter of a few hours, depending on such factors as target size and the thermal conductivity of the shell material. Redistribution rates found using the 2D code mentioned above are shown as a function of shell wall conductance in Figure 6.4.2-5. The relatively low thermal conductance of the CH shell means that

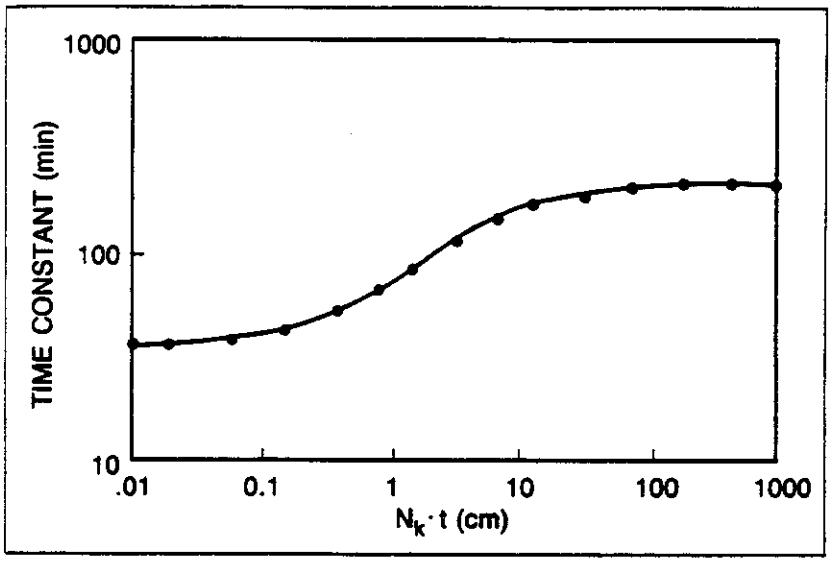

Figure 6.4.2-5. The Thermal Conductivity of the Shell Material Is an Important Factor in Determining the Rate of Heat Transfer. N_k is a Factor Used to Normalize the Thermal Conductivity of the Shell Material to that of Glass.

predicted e-folding time constants will fall on the left side of the curve in the figure. Experimental results obtained using a thick-walled copper cylindrical with sapphire windows bear out these optimistic theoretical predictions.[30] DT ice redistribution due to beta heating within a 5.74 mm enclosure led to nearly uniform layers within three hours. Faster rates can be expected with actual targets due to the low thermal conductivity of CH compared to copper.

The target factory design proposed here in allows four hours for the beta layering step, a time that seems reasonable in view of the available evidence and the possibility of creating reasonably uniform layers by such preliminary steps as air tumbling.

6.4.2.4 Indirect Drive Target Case Fabrication and Mating - The capsule for indirect drive targets will be similar to the direct drive targets, and will be fabricated and filled in the same way. The radiation case must then be mated to the capsule under cryogenic conditions. Incorporated in the case is a support structure to provide target position and ability to survive acceleration while providing good illumination symmetry. This configuration also happens to be the best for target performance and would be easiest to manufacture. The exact configuration chosen will depend on target performance requirements, which are beyond the scope of this report. However, it should be possible to cheaply mass produce targets in either configuration.

Indirect Target Engineering Model - After the project decision to use the indirect drive (ID) target as the baseline target for the heavy ion driver, a study was conducted to determine the feasibility of mass producing the targets, techniques of handling and injecting the target, and the survivability of the target. Indirect laser targets have been successfully used in experiments, but only on a single shot basis, perhaps suspended or positioned on a pedestal within the test chamber. Care was taken in the fabrication of these limited-production targets to obtain the performance or experimental results desired. Likewise, the thermal and handling environments were tailored to minimize design and physics constraints.

To date, there has been no need to propose or design a mass-produced, commercial, indirectly-driven fusion target as it is not needed for the present or planned experiments. Therefore, to determine within this unclassified study the engineering feasibility of an indirectly-driven target, not the physics feasibility, an engineering model was proposed for evaluation and study.

General Target Model Guidelines - The indirect target is designed for the heavy ion driver system although the design could easily be adapted to the laser driver system. The DT capsule contained within the outer case is similar to direct drive capsules. The outer radiation case enclosing the DT capsule is assumed to be cylindrical with energy converter regions located on the two ends of the heavy ion target case. A laser indirect target would have apertures on the two ends instead of the energy converter regions. The target would be injected into the reactor cavity along its longitudinal axis with an induced spin to provide stabilization.

The Target Working Group (TWG) considered both single- and double-sided illumination schemes for the heavy ion, indirectly-driven target.[1,2] However, the TWG felt the two-sided target should be employed as the baseline because of the speculative nature of the single-sided illumination.[2] Thus two energy converter regions will be used, one in each end of the cylinder on the axis of symmetry. The TWG-supplied heavy ion ID gain curves,[1] shown in Figures 3.3-8 and 3.3-9, indicate focal spot sizes from 4 to 10 mm in diameter, depending on the ion range (R) and driver energy chosen. For the driver design point chosen, the converter region geometry was determined. This converter geometry allows for some beam misalignment with respect to the target. An engineering model of the converter region was defined. The converters will be affixed to the inner surface of the radiation case. One of the engineering analyses addressed the question of the minimum thickness of the radiation case to withstand the acceleration forces of the injection systems, which was tentatively chosen to be 100 g's for the indirect target. The case geometry is configured to ease fabrication and reduce stress concentrations. If target physics constraints would require other configurations, these features could easily be changed.

The initial effort was to determine if the acceleration loads of 100 g's would cause buckling or distortion of the case walls or ends. The dimensions of the case were held to the minimum to reduce the hydrogen and carbon gas load to be introduced into the cavity. As the ion beams interact with the energy converter region, soft x-rays are created and bathe the inside of the case and the DT sphere. To efficiently contain the X-ray radiation, lead was chosen for use in the case to be compatible with the wall protectant.

The central capsule should be supported so as not to significantly disturb the illumination of the capsule. For the calculations as to the elastic strength of the case walls, the weight of the central capsule was transferred to the walls, but the mass of the support was neglected. The mass of the case walls, converter regions, and the support mechanism was estimated.

For the target to have the proper thermal conditions when it reaches the center of the cavity, the entire target must be at cryogenic temperatures up to and including the injection operation. During a preliminary investigation, no CH compounds were found to exhibit adequate structural properties at these cryogenic temperatures. Other materials that can easily withstand the operating environment with adequate structural properties may not be suitable from a physics standpoint and desirable additions would not be attractive from a materials handling standpoint. However, specific structural properties were used as representative of an improved CH plastic to be engineered for this application.

Radiation Case Wall Structural Analysis - A Nastran finite element model was constructed with 1155 nodes, 1155 QUAD elements, and 36 TRIA elements to model the case. For the wall thickness trade study, the internal DT capsule was represented as a point mass in the center of the case with a structure carrying the load to the case walls. The analysis was conducted using a Nastran inertial relief analysis method. A pressure of 3.3 kPa (0.47 psi) behind the target will impart approximately 100 g's acceleration. The maximum case wall stress is 0.079 MPa that is well within the allowable limits of the material. Thus the case can easily withstand the acceleration load of 100 g's.

The internal support structure was more difficult to postulate and analyze. Room temperature stress properties were used to estimate allowable designs based upon capsule survivability during acceleration and resultant deflection and vibration modes. An increase in the thicknesses assumed may be dependent upon the cryogenic allowable stress levels in the to-be-determined material. In the search for suitable materials for this engineering study, the choice was limited to available commercial materials. It was found this material will easily withstand the imposed acceleration stresses and the resultant vibrational displacements would probably be acceptable even at cryogenic temperatures. The deflection was predicted under full acceleration

loading. The calculated natural frequency of the capsule is approximately 1500 Hz. Assuming a conservative damping coefficient of 0.1% (low damping), the capsule would oscillate within the case approximately 75 times during the transit of 10 meters from the end of the injection system to the center of the reactor chamber (50 ms). With this damping coefficient, the amplitude at T = 0 would be negligible.

Summary of Indirect Target Structural Analyses - An engineering model of the indirect drive (ID) target was defined using commercially available materials. Structural analysis of this model indicated the outer radiation case wall would easily withstand the desired acceleration loads of 100 g's. An acceptable structural support technique is proposed provided adequate structural properties can be obtained in suitable materials. For the materials and properties assumed, the stresses and deflections were within acceptable engineering limits.

Summary of Indirect Target Material Requirements - The above engineering target model provides baseline data for the material's usage and waste product generation within the reactor cavity.

Fabrication of the Indirect Target - The manufacturing process for the indirect target is designed to support a pulse rate of the heavy ion driver reactor of 3.5 pulses per second. The operations are divided into ambient and cryogenic processes as is indicated in Figure 6.4.2-6. Duplicate facilities with excess capacity are planned to reliably produce the required quantities. Buffer queues are also planned to assure 100% target availability for the reactor. The reactor will require 12,600 targets per hour or 300,000 per day. The rates of production and cryogenic atmosphere necessitate inclusion of the inspections into the automation scheme. In the interest of minimizing the tritium inventory, a Just In Time (JIT) inventory philosophy is anticipated using a partnership with the supplier to provide the safety stock required.

The design of the target lends itself to the fabrication techniques employed in the pharmaceutical industry, although somewhat larger in diameter. The case will be fabricated in two half cylinders to allow the tritium capsule to be attached with its support structure centered in the cylinder. Several alternatives are available to close the case. One alternative is to store the right half of the case at room ambient and slide it over the section with the capsule that will be at cryogenic temperature. The subsequent shrinking of the material as it approaches the cold temperature will create a bond. Two other alternatives address bonding the two sections together. The application of ultra sonic welding is a viable candidate. The energy is applied to the point where bonding is required and a localized rise in temperature results that creates a bonded butt joint. The other alternative is to rotate the mating bodies in opposite directions and create an inertial weld of the butted surfaces. Both alternatives would require the buffer stores in the cryogenic environment to have temperature stability.

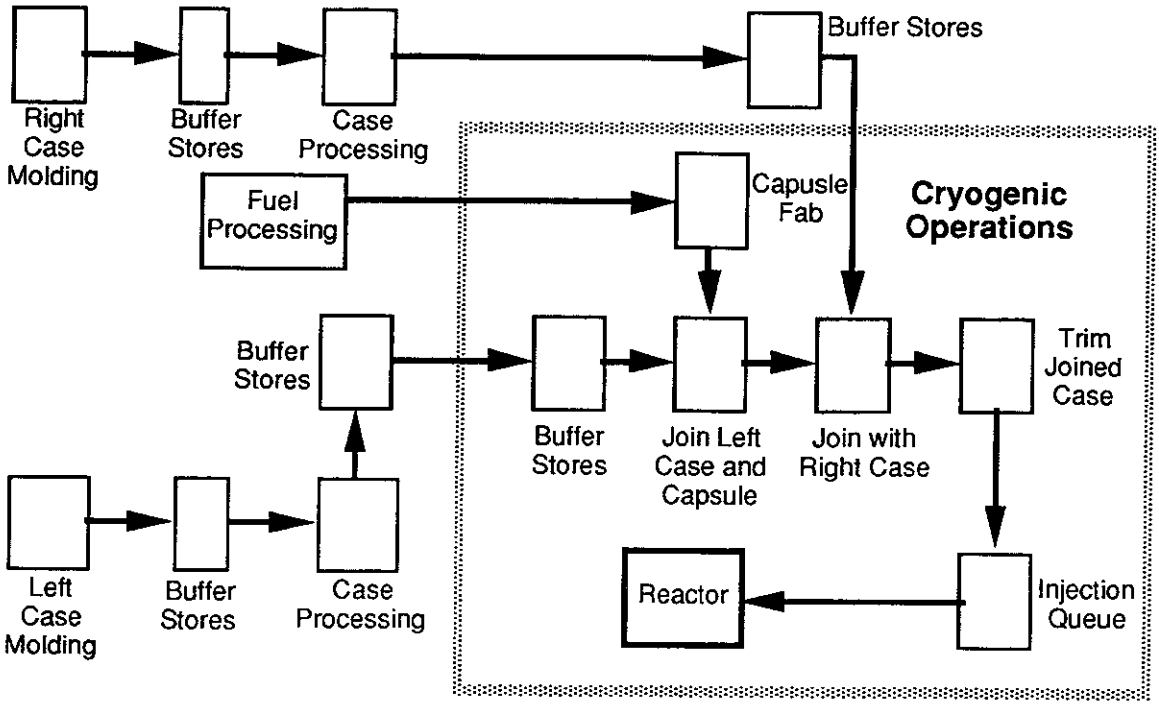

Figure 6.4.2-6. Indirect Target Production Process

The fabrication of the case sections would be done in multi-cavity molds. The half cylinders would be formed with an extrusion or blow molding process that would hold the tolerances on the diameter to a few thousandths of an inch and wall thickness to a fraction of a thousandth of an inch. The cylinder ends can be trimmed to the desired length. The extrusion die would be designed to form the converter section and the constant thickness walls. With molds of 100 cavities and the short cycle time, the utilization would be less than 12 hours per day that would allow ample time for machine and mold maintenance. Space cavity inserts and the possibility of operating with missing cavities would assure adequate supply. A 24 to 36-hour buffer stock would be adequate. The availability of two machines, one dedicated to each half, would provide further insurance against a stoppage.

The vapor deposition facilities will require special fixturing for multi-unit processing. The number of units has not been determined but, based on other applications, a minimum of three work cells would be required. These ambient temperature operations need to be adjacent to the cryogenic operations since the lead will be recovered from the reactor exhaust stream and reused in this process. The facility design will be required to prevent lead escaping into the atmosphere inside the ambient room as well as to the exterior.

The fuel capsule will be manufactured in a process similar to the laser direct drive target, of similar materials. A diffusion process will be used to fill the capsule with DT. The capsules will be fabricated and inspected in a JIT process for injection to minimize

the tritium inventory. Multiple parallel production lines will be utilized to assure the necessary reliability values.

The DT capsules will be mated initially with one half of the radiation case and the capsule support structure in the cryogenic environment. The assembly of the remainder of the case will occur in the next work cell using one of the proposed methods of attachment. The next work cell will deflash (trim) the cases, if necessary, and load them into a transportation fixture for the injection queue.

The equipment design specifications will provide for in-process inspection internal to the equipment with attribute data acquired for process control purposes. Appropriate "no touch" measurement techniques such as laser micrometers or air gaging will be used for data acquisition. Built in processors would provide continuous statistical analysis of the output. The initial designs will be built around a requirement that 35% of the work stations in any piece of equipment be available for future growth to provide flexibility for future changes to the process and unanticipated problems.

6.4.3 Target Factory Definition - Targets for inertial fusion experiments conducted to date have been hand crafted at great expense in time and money. Occasionally, single targets are made with precise individual features such as surface bumps, thin coatings of exotic materials and doping with trace elements. Production methods in target factories for future IFE reactors will be radically different. These factories will need to economically mass produce hundreds of thousands of standardized targets per day. At the moment there is not even general agreement on what fabrication methods will be most appropriate or even, in the case of indirect drive, what the targets will look like. Nevertheless, there is good reason to believe that this technological challenge can be met. Reactor targets will be small and complex. It will be necessary to built them to exact specifications. Experience in other industries shows us that novel products with all of these characteristics can be produced economically. Semiconductor chips, for example, have even smaller features that must be cheaply fabricated to similarly demanding specifications in hundreds of thousands of copies. Similar examples can be cited in industries producing everything from electronic equipment, pharmaceuticals, and small mechanical devices, to optical equipment and even toys. Obviously, in our present state of technological uncertainty, the advances of tomorrow can quickly make the designs of today obsolete. Nevertheless, it is still useful to consider the general layout, potential fabrication and inspection steps, special safety and containment precautions and approximate staffing requirements of future target factories, if only to make the case that mass production of reactor targets is possible and can be done cheaply enough to make fusion power economically attractive.

6.4.3.1 General Factory Layout - The target factory concept for direct drive targets will be discussed first. Many of the production steps for direct drive targets will be found in the indirect drive target factory as well. Operations peculiar to the indirect drive factory will be discussed in a separate subsection.

The proposed target factory will be separated into two distinct sections. Operations requiring the handling of tritium will be carried out in one section, referred to hereafter as Zone II, and all other production steps in the other section, referred to as Zone I Gross dimensions of both sections will be approximately 50 m x 50 m. Figure 6.4.3-1 shows the functional relationships between the major operations requiring space in the factory. It is, of course, premature to consider detailed architectural planning at this point. However, the general layout of Zone I is expected to reflect the diagram in Figure 6.4.3-1 to the extent that actual production steps, which are shown in the large rectangle, will be carried out in a large, central bay area. All other operations, such as administration, maintenance, etc., will be carried out in peripheral areas. This arrangement will allow the greatest flexibility in accommodating changes in production steps due to technological improvements in materials, fabrication techniques, etc.

The majority of the resources in terms of space and manpower in Zone I will be devoted to production and delivery of finished target shells to Zone II. In addition, significant resources will be devoted to inspection and recycling of used sabots and fabrication of new ones to make up for normal attrition. Finally, Zone I will contain facilities for production of radiation case elements for indirect drive targets. All production steps will be carried out in a number of parallel lines that will provide redundant capacity to allow periodic maintenance of individual line elements and, if necessary, production of targets for other facilities.

The basic technologies chosen for target shell fabrication are dual-nozzle droplet generators combined with microencapsulation. As already pointed out above, production of significant numbers of reactor size targets has not yet been demonstrated with this combination of technologies. In spite of this, their choice does not necessarily entail any technological leap of faith. They are certainly capable of producing the large numbers of target shells required for reactor operations. If significant resources are devoted to research and development in this area, it is not unlikely that variations will be found which are capable of turning out target shells with the required thickness and size. Even in the event that no such process is found, these methods can be used in combination with shell coating and micromachining steps to produce reactor-size targets. The question is whether they can do it economically. The evidence from many other industries where demand has led to the inexpensive manufacturing of small and complex items suggests that they can.

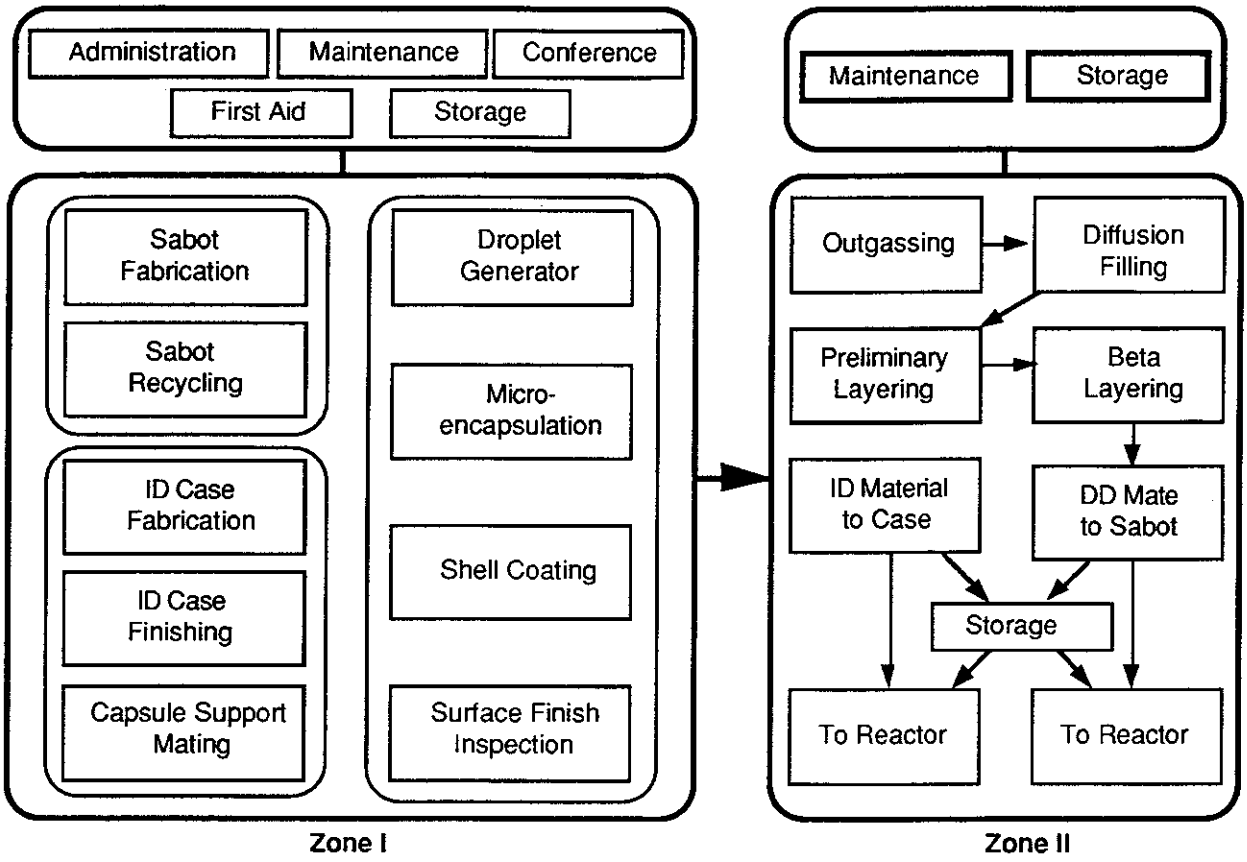

Figure 6.4.3-1. Functional Relationships for Buildings in Target Factory

At the moment, no need is foreseen for coating steps other than those required for fabrication of the main shell. The target prescribed by the TWG has no additional elements required by any peculiarities of the reactor design proposed here. The open bay design of Zone I could accommodate such steps if necessary; however, finished target shells will be subjected to a final heating and outgassing step before delivery to Zone II or vacuum storage.

In addition to fabrication of the main target shell, provision is made in Zone I for reception and inspection of used sabots from the target injection system and production of new sabots to replace those damaged or worn. Sabots will be used only for direct drive targets. Indirect drive targets are completely enclosed in a radiation case that will provide sufficient protection to the target capsule during the acceleration process. Sabots are considered precision parts in this design. An example is shown in Figure 6.4.3-2. The target will be seated loosely in the nose of the sabot. The sabot must be designed so as not to damage the capsule or impart a transverse velocity component to the target on release of the capsule. Sabots will be injection molded of thermoplastic and then finished by machining with high tolerance tools. The

ferromagnetic material shown in Figure 6.4.3-2 will be mechanically attached to the sabot. It is expected that sabots will be reused an average of 20 times.

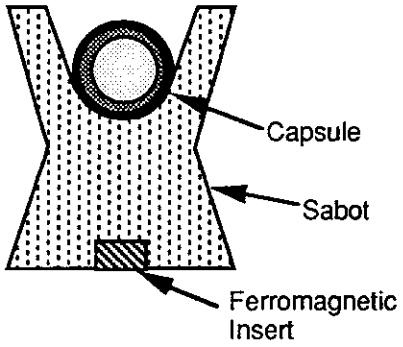

Figure 6.4.3-2. Direct-Drive Sabots Must Be Precisely Machined to Insure a Straight Trajectory for the Loosely Seated Capsule

Finally, indirect drive cases and auxiliary parts will be produced in Zone I. Indirect drive cases are not considered precision parts. However, they must be made to reasonable tolerances as they will be in direct contact with the injection system barrel during target injection. The left and right radiation case components will be molded. Finally, capsule support structures will be attached to the open ends of both case components to provide support for the target capsules. As shown in Figure 6.4.3-1, all components produced in Zone I will then be transferred to Zone II for DT fueling operations.

Zone II will be designed to provide for tritium containment and all systems therein will be designed to operate with as little human intervention as possible. Application of artificial intelligence and robotics will be used in all production and inspection steps. The need for a human presence in Zone II will be limited, as much as possible, to provision for periodic maintenance. High pressure and cryogenic barriers in Zone II are as shown in Figure 6.4.3-3.

Target capsules arriving in Zone II will be introduced into diffusion filling vessels such as the one shown in Figures 6.4.2-3 and 6.4.3-3. Four to six of these aluminum vessels will operate in parallel to provide redundant capability to provide for standard maintenance and continuous plant operation in case of failure of any of the vessels. The target capsules will be mechanically conveyed through internal locks in the vessels to allow for gradually increasing external DT pressure and maintaining optimum filling rates. Optimum fill temperatures of around 100°C will be maintained in the vessels with the aid of external heating and cooling elements. Depending on the exact size and polymerization of the target capsules, diffusion filling will take from 24 to 36 hours.

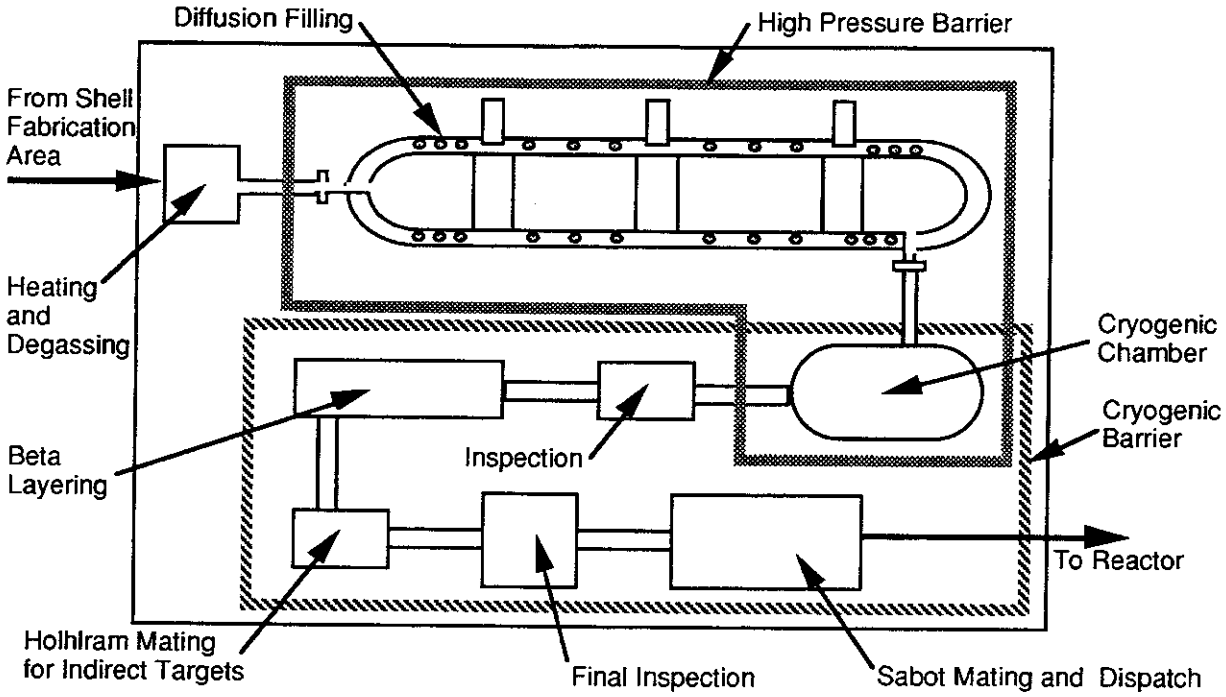

Figure 6.4.3-3. Zone II Layout for Direct and Indirect Drive Targets Shows High Pressure and Cryogenic Barriers

After diffusion filling, capsules will be removed to separate containment vessels and cooled to cryogenic temperatures. This could be done in a high pressure DT environment if necessary to prevent excessive fuel loss due to outgassing during the cooling process. The ambient gas would be cooled to near cryogenic temperatures with the target capsules and pumped off at the appropriate time.

At this point, indirect drive target capsules would be mated to their radiation cases. This process will take place at cryogenic temperatures using precooled parts. Ideally, case components will be fabricated with sufficient accuracy to lock firmly together, holding the capsule in place.

Direct drive targets will be suspended between layers of thin (<1.0 mm) plastic film and also be cooled with gaseous helium during the beta layering step. Next, they will be mated to their sabots. At this point, both types of target will normally be delivered to the reactor for immediate injection. Some provision will be made for short term storage, but the shelf life of the targets is expected to be quite short (<100 hours) due to radiation damage to the inner surface of the CH shell and it will be necessary to thermally isolate them during storage.

Inspection of Target Components - Inspection of components will take place after all major target fabrication steps. In principle, inspection of parts such as sabots and indirect drive case elements could be done visually by a staff of inspection personnel. However, this would be expensive and, in the case of opaque components such as

target shells, impractical. Fully automated inspection with the aid of artificial intelligence and pattern matching and recognition techniques is preferred. Limited application of such techniques has already been demonstrated in the field of optical interferometry for glass shells, as shown in Figure 6.4.3-4. For opaque parts, x-ray microscopy is proposed.[32,33] This technique lends itself to batch target characterization, and is capable of detecting target flaws at the submicron level.

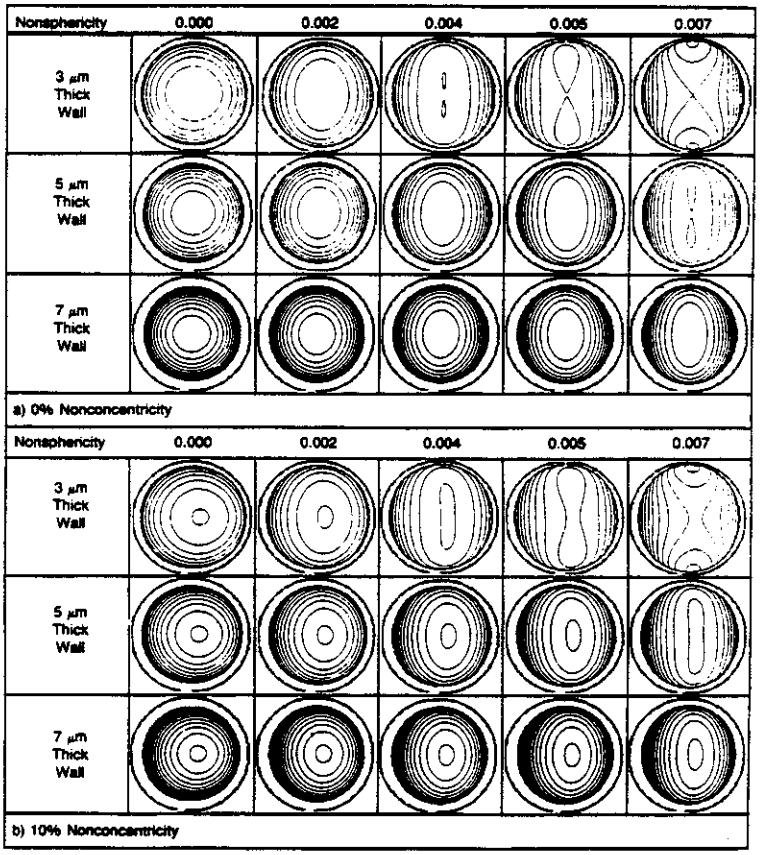

Figure 6.4.3-4. Computer Generated Interferometric Reference Patterns Suggest the Possibility of Mass Inspection with the Aid of Pattern Matching and Artificial Intelligence

Target Costs - Target costs are estimated according to a model proposed by Pendergrass, et. al.[34] In this model, costs are divided into three components: target factory capital charges, nontritium materials costs, and nonfuel, nonmaterials O&M costs. Simple algorithms are supplied for computing these costs that depend on a number of fixed parameters as well as variables intrinsic to individual reactor designs. Default values supplied for the parameters have been used here unless otherwise noted. Appendix C, Section C.3.7, has more detail on the nominal capital costs, repetition rates, and reject fractions used to arrive at the final cost values.

The form of the capital cost model is

$$C_F = \sum_{i=1}^{N_s} C_{FRi} \left(\frac{P_{Ai}}{P_{AR}} \right)^{a_i}$$

Eq. 6.4.3-1

where C_F is the total target capital cost (M$), C_{FRi} is the reference capital cost increment for the target factory section to manufacture target substructure i (M$), N_S is the number of substructures, P_{Ai} is the required annual production capacity for the section of target factory that produces target substructure i (1/yr), P_{AR} is the reference annual production capacity of the target factory (10^8/yr), and a_i is a production capacity scaling exponent of the section of the target factory to manufacture target substructure i. The Pendergrass model distinguishes between two inspection models, depending on whether inspection takes place of each major target component as it is completed or only of finished targets. For the designs proposed here, the first model is appropriate. The target rejection model for this type of inspection is

$$P_{Ai} = \frac{P_A}{\prod_{k=i}^{N_s} (1-F_k)}$$

Eq. 6.4.3-2

where P_A is the design target factory annual production capacity and F_k is the fraction of targets rejected for failure to meet specifications for target substructure k. For the direct drive reactor, there are two significant target substructures: the single-shell target fuel capsule and the sabot. A reference capital cost of $122M (escalated to 1991$) was given for the target shell manufacturing facilities. No value was given for the sabot manufacturing. Capital costs for the sabot should be much lower in view of the simplicity of the design and the potential for reuse of sabots. C_{FRi} for sabots was asssumed to be $5M for a total nominal capital cost of $127M. The default rejection fraction for the fuel capsule of 0.02 was used, and a sabot rejection fraction of 0.01 was assumed. Substituting the Prometheus laser option values of repetition rate into Eq. 6.4.3-1 yields:

C_F(direct drive) = $134.92M

Sabots are not required with the indirect drive targets. Instead, a radiation case with energy convertor regions is used. The nominal capital cost for this element is assumed to be $37M. A nominal captial cost of $145M is assumed for the fuel capsule

that may be somewhat more complex. The nominal capital for the indirect drive target totals $182M. The default rejection fraction of 0.02 is assumed for the radiation case. The added energy convertors contributes an additional 0.01 rejection fraction. The fuel capsule default rejection rate is retained at 0.02. Again, substituting these values into Eq. 6.4.3-1 yields:

C_F(indirect drive) = $143.62 M

Materials costs for both designs are insignificant in view of the inexpensive choice of target materials and the possibility of recycling the lead in indirect drive radiation cases. Pendergrass et. al. give reference materials costs of 0.015 and 0.025 $/target for direct and indirect drive laser targets expressed in 1986$. For the designs proposed here, these numbers are much too high. It was assumed the laser direct drive materials costs are $0.010 per target and the HI indirect drive materials costs are $0.014 per target. Refer to Appendix C for the relevant cost estimating relationships. Heavy ion target materials were higher due to the addition of the energy converter structures.

Nonfuel, nonmaterials O&M costs include personnel costs, the annual target factory interim replacement cost, annual maintenance materials cost and O&M cost for other supplies and materials. The algorithm used to determine personnel costs is

$$C_p = (0.001\ \text{k\$/M\$}) \sum_{j=1}^{N_{JC}} N_{Rj} C_{PRj} \left(\frac{P_A}{P_{AR}} \right)^{d_j} \qquad \text{Eq. 6.4.3-3}$$

where N_{JC} is the total number of job categories, N_{Rj} is the reference number of persons required for a job category, C_{PRj} is the reference annual cost per employee in job category j, and d_j is the exponent for scaling of number of staff required for job category j (1.0 if category scales, 0.0 if not) with design target factory annual production capacity. Some of the data used in the above equation are shown in Table 6.4.3-1. The format and defaults in Reference 36 have been used in the table where appropriate. However, some modifications are introduced which reflect the idiosyncrasies of the design presented here.

Table 6.4.3-1
Target Factory Staffing Requirements (10^8 Targets/Yr)

Position	Salary 91$	Plant Staff Capsule		Rad Case	Indirect Drive O&M		Direct Drive O&M	
		Fixed	Scalable	Scalable	Fixed	Scalable	Fixed	Scalable
Plant Manager	82.8	0.5			41.4	0.0	41.4	0.0
Secretary	29.8	1.0			29.8	0.0	29.8	0.0
Clerk Storekeeper	30.3	1.0			30.3	0.0	30.3	0.0
Auditor Bookkeeper	38.6	1.0			38.6	0.0	38.6	0.0
Janitor	22.4	1.0			22.4	0.0	22.4	0.0
Target Mfg Specialist	55.1	2.0			110.1	0.0	110.1	0.0
Quality Control Engineer	55.1	1.0			55.1	0.0	55.1	0.0
Electrical Engineer	55.1	0.5			27.5	0.0	27.5	0.0
Mechanical Engineer	55.1	0.5			27.5	0.0	27.5	0.0
Chemist	55.1	2.0			110.1	0.0	110.1	0.0
Health Physicist	55.1	1.0			55.1	0.0	55.1	0.0
Laboratory Technician	32.3	6.0		1.0	193.8	82.8	193.8	0.0
Shift Supervisor	60.1	2.5			150.3	0.0	150.3	0.0
Senior Operator	51.2	5.0			255.9	0.0	255.9	0.0
Operator	46.8		5.0	5.0	0.0	468.3	0.0	234.1
Assistant Operator	41.4		5.0		0.0	206.9	0.0	206.9
Maintenance Supervisor	46.8	2.5			117.1	0.0	117.1	0.0
Mechanical Maint Tech	41.4		5.0	2.5	0.0	310.4	0.0	206.9
Electrical Maint Tech	41.4		5.0		0.0	206.9	0.0	206.9
Inst. & control Maint Tech	41.4		5.0		0.0	206.9	0.0	206.9
Quality Assurance Tech	41.4		5.0	2.5	0.0	310.4	0.0	206.9
Security Specialist	34.0	5.0			170.0	0.0	170.0	0.0
Peak Maint FT Equiv	48.0		5.0	2.5	0.0	360.3	0.0	240.2
TOTALS					1434.9	2102.3	1434.9	1508.9
						3537.3		2943.8

Use of the above numbers for personnel cost estimation gives

C_P(direct drive) = \$4.15M/yr
C_P(indirect drive) = \$3.91M/yr

The algorithm for annual target factory interim replacement cost is,

$$C_{IR} = F_{IR}C_F \sim \$1.35M \text{ (DD)}, \sim \$1.44M \text{ (ID–HI)} \qquad \text{Eq. 6.4.3-4}$$

where F_{IR} = interim replacement annual cost factor, with a default of 0.01. In addition to the above, the annual maintenance materials cost,

$$C_{MM} = F_{MM}C_{MP} = \$6.22M \text{ (DD)} = \$5.85M \text{ (ID–HI)} \qquad \text{Eq. 6.4.3-5}$$

where F_{MM} is a maintenance materials cost factor with a default of 1.5 and C_{MP} is total annual maintenance personnel cost computed using a formula analogous to Eq. 6.4.4-3, and the reference fixed annual cost for supplies and expenses O&M costs is

$$C_{SE} \sim \$0.6M/\text{year} \qquad \text{Eq. 6.4.3-6}$$

6.4.4 Target Injection and Tracking - Injection systems capable of firing multiple targets at rates greater than those needed for IFE reactors have already been in existence for several years. They were designed to refuel tokamaks in the magnetic fusion program.[35,36,37] Magnetic fusion injection systems have shown that cryogenic pellets can be injected at the velocities and repetition rates required in IFE reactors. Many target injection techniques developed for magnetic fusion may eventually find application in inertial fusion. However, significant differences exist between the two approaches to fusion in the requirements they place on target injection systems. The pellets used in magnetic confinement systems are merely chunks of solid H_2 or D_2. The goal is to accelerate them to extremely high velocities, enabling them to penetrate to the center of the tokamak plasma. They are significantly more tolerant of high acceleration and surface abrasion than inertial fusion targets, and there is no need to delicately synchronize their velocities with a system of laser or particle beams. Target injection systems are presented here for the direct and indirect versions of Prometheus which address the technological challenges unique to each system.

6.4.4.1 Direct Drive Target Injection System - Choice of a direct drive target injection system is conditioned by the fact that it will probably be necessary to deliver direct drive targets in a sabot. Unprotected targets would be subjected to unacceptable levels of surface abrasion and thermal gradients during acceleration. Assuming a sabot is necessary, such questions must be answered as how to separate the target from the sabot prior to injection into the reactor cavity and how to recover the sabot for reuse. In addition, the synchronization and tracking problem inherent in IFE must be solved. An electromagnetic acceleration system is proposed as the best option for meeting these technological challenges.[38]

An example of the proposed direct drive target and sabot and a schematic of the injection system is shown in Figure 6.4.4-1. Targets will arrive from the target factory already mounted in their sabots. The sabot end cap is designed only to protect and hold the target in place during transit from the factory to the reactor, and will be removed shortly before the target is fired. Targets in both the DD and ID designs will be accelerated to 200 m/sec. The direct drive target will be injected through the first wall at a point about 7.5 meters from the beam aiming point. The target will traverse the cavity in approximately 37 msec. The target will enter the cavity about 140 msec after the previous shot, a sufficient time for cavity temperature and pressure to fall to levels which will not adversely affect the target (see Section 6.4.1.2). The injection system will have a 2-meter long injection module as shown in Figure 6.4.4-1. The module will be synchronized to provide the design repetition rate of 5.65 Hertz. Accelerations of about 1000 g will be imparted to the direct drive targets. Solid D_2 pellets have withstood accelerations of 5×10^6 g without breaking,[39] suggesting that thick DT shells such as those shown in Figure 4.6.1-1 will easily withstand accelerations more than three orders of magnitude smaller.[40] However, the situation is complicated by the strong dependence of the yield stress of solid hydrogen on

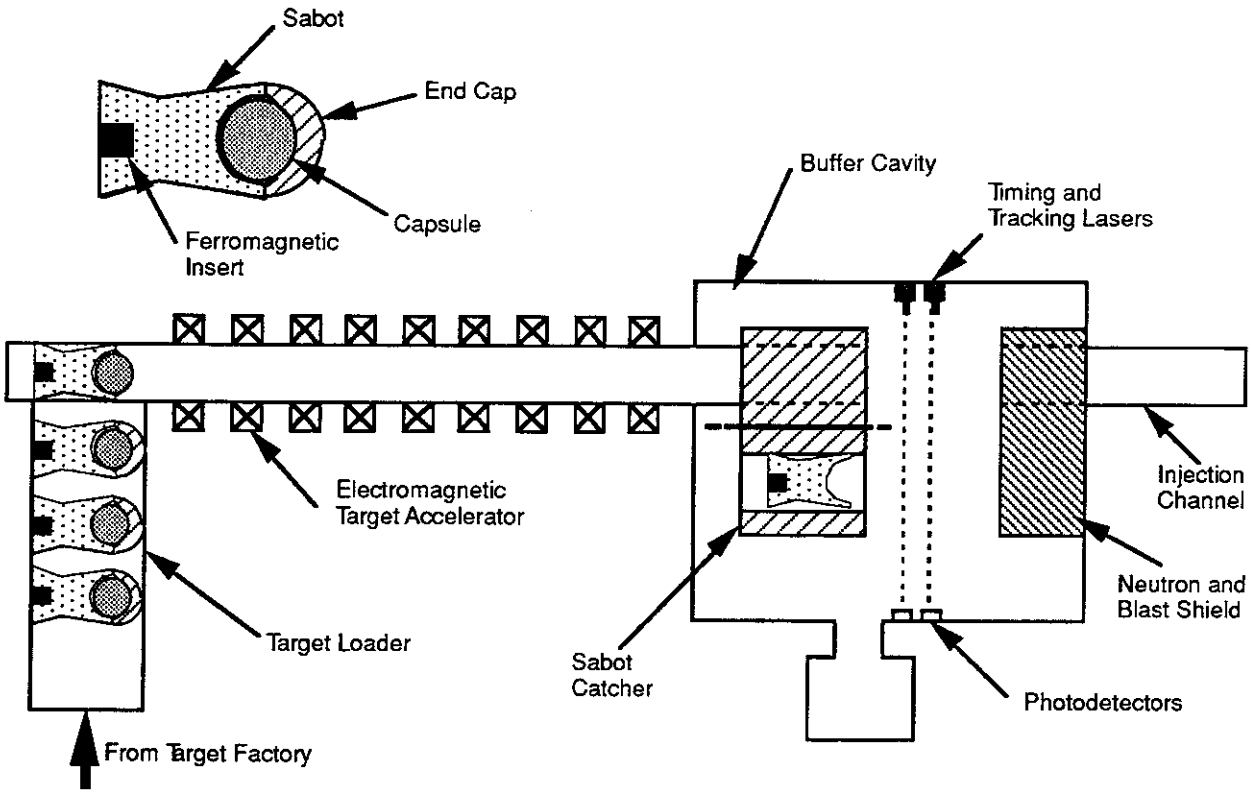

Figure 6.4.4-1. Schematic of One of the Eight Direct Drive Pellet Injection Modules

temperature. The solid targets mentioned above were at temperatures of about 12K. Yield stresses for solid hydrogen near the triple point are much less.[41] It is assumed here that fuel temperatures of less than 15K are acceptable.

Acceleration will take place on the principle of a linear synchronous motor, and a number of ferromagnetic materials exist which are capable of accelerating the target and sabot to 200 m/sec over a distance of two meters assuming achievable mean effective gradients $\delta_x B$ of the magnetic induction B of the accelerator coils of around 100 T/m.[38] The system has the advantage of requiring no medium in the barrel unlike railguns and, of course, pneumatic systems.

The injection system for the direct drive target will be mounted at the top of the reactor cavity, injecting downward into the cavity, as shown in Figure 6.4.4-2. After leaving the injection system barrels, targets will pass through a sabot catcher into a diagnostic chamber. There, a system of optical interrupters will be used to transmit position and timing information to the driver beams. Such systems are already in use in magnetic fusion pellet injection systems.[42,43] Timing information will be provided by a pair of light barriers or beams through which the target must pass on its way to the reactor cavity. Directional information, i.e., data on how far the target will deviate from a

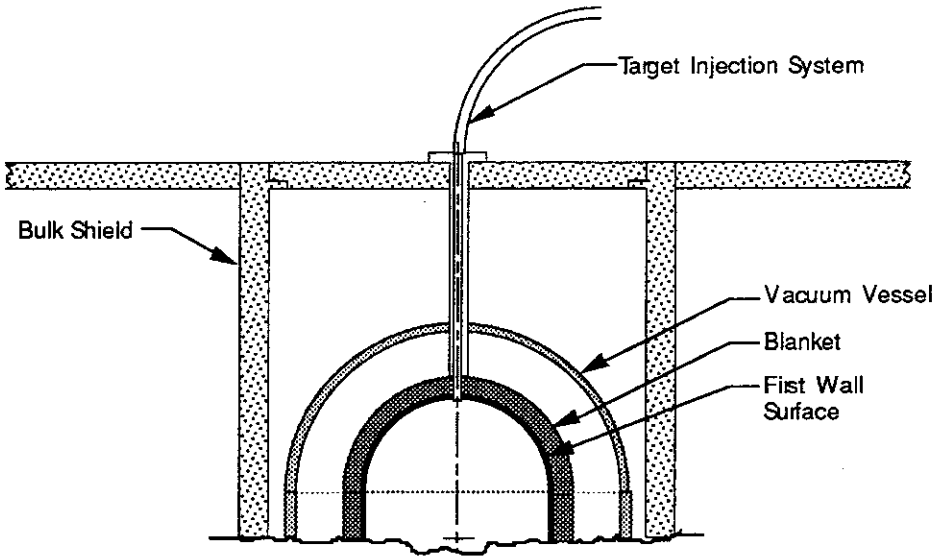

Figure 6.4.4-2. Electromagnetic Direct Target Injection System Employed in the Laser-Driven Reactor

straight line path, will be provided by interrupters oriented orthogonal to each other and to the target's direction of travel. In one such system devised for cylindrical targets which might be adapted for spherical targets, white light is broken down into a spectrum across the target path.[44] The parts of the spectrum interrupted by the target provide data on its exact location. It will be possible to steer the beams to hit targets within a radius of a few millimeters from the nominal aiming point on a shot to shot basis. Since targets must hit within this volume after leaving injector barrels located over ten meters away, it will be necessary to keep the transverse and longitudinal velocity scatter to a few millimeters per second. This requirement will be challenging with targets which are accelerated while seated in a sabot. It will be necessary to manufacture the sabots to precise specifications and inspect them after each shot. They will be decelerated before reaching the sabot catcher to prevent excessive impact damage.

The injector barrel will be enclosed in a thermal jacket and cooled by a continuous flow of helium. A number of similar systems for cooling barrels of magnetic fusion pellet injectors are described in the literature.[45]

6.4.4.2 Indirect Drive Target Injection System - Injection of indirect drive targets is complicated by their inherent fragility. Ideally, the target capsule would be suspended within the radiation case without any support structures whatsoever. Unfortunately, this is impractical in the real world. As disussed in Section 6.4.2.4, these capsules must be supported with a light weight structures, compatible with the required target physics and be capable of withstanding an acceleration of 100 g's. In

order accelerate targets to the optimum velocity of 200 m/sec, injection system barrels approximately 20 meters long will be necessary.

Indirect drive targets enjoy some inherent protection from friction and overheating because they are completely enclosed in radiation cases. Sabots will, therefore, not be used with the HI design. Pneumatic acceleration has been chosen in order to eliminate the need for ferromagnetic or other special materials in the target's radiation case. Numerous pneumatic pellet injection systems capable of repetitive injection have been built for fueling tokamaks, and their technology is, consequently, significantly more mature than that of competing electromagnetic systems. Their major drawback is the need for a propellant gas.

Ideally, the longitudinal axis of the heavy ion indirect drive target should be aligned with the two diameter, two HI beam sets. Unfortunately, the final focus coils prevent coaxial injection. Instead the injection system will be aligned 10° off the horizontal beam axis. A diagram of the indirect drive injection system is shown in Figure 6.4.4-3. An eight barrel system will be used. This will provide sufficient time for each barrel to be reloaded, fired and evacuated while maintaining a repetition rate of 3.54 Hertz. The barrels will be fired by electronically opening a magnetic valve[46,47] to the D_2 propellant gas reservoir, as shown in Figure 6.4.4-4. A piston in the reservoir will maintain constant accelerating pressure behind the target during its approximately 0.2 second trip down the barrel. Its movements will be controlled by automatic interpretation of data from a quartz pressure transducer mounted in the propellant gas cavity. An advantage of the requirement for low acceleration is that it allows the use of cold propellant gas. Thus, a potential source of target overheating is avoided.

A problem inherent in pneumatic injection systems is how to avoid contaminating the reactor cavity with propellant gas. Fortunately, the magnetic fusion community has already provided many of the answers on how to deal with this problem.[48,49] Piezoelectric pressure transducers will be mounted along the length of the barrel to sense the passage of the target. This information will be relayed to gate valves on the muzzle of each barrel.[50] The gate valve will be closed immediately after passage of the target, and the propellant gas in the sealed barrel will then be pumped out.

After leaving the injector barrel and passing through the diagnostic chamber, targets will travel ballistically down guide tubes through the bulk shielding, blanket and first wall. These will be slightly curved to account for the drop in the trajectory due to gravitational forces on the way to the aiming point.

Indirect drive targets must be properly oriented during beam illumination of the energy convertor regions. It is therefore necessary to impart a spin to them to prevent them from tumbling. This will be accomplished by rifling the injector barrels. Small tabs will be molded on the radiation cases to accept the rifling.

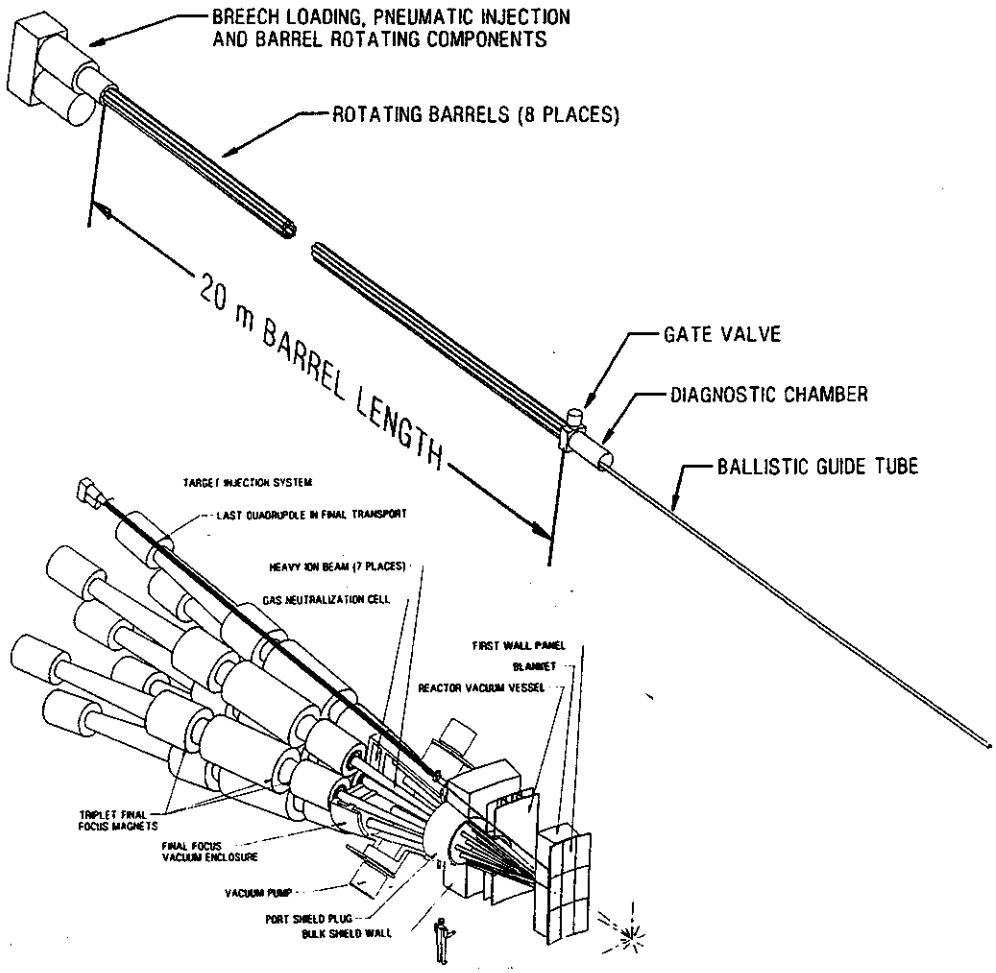

Figure 6.4.4-3. Pneumatic Indirect Target Injection System for Heavy Ion-Driven Reactor

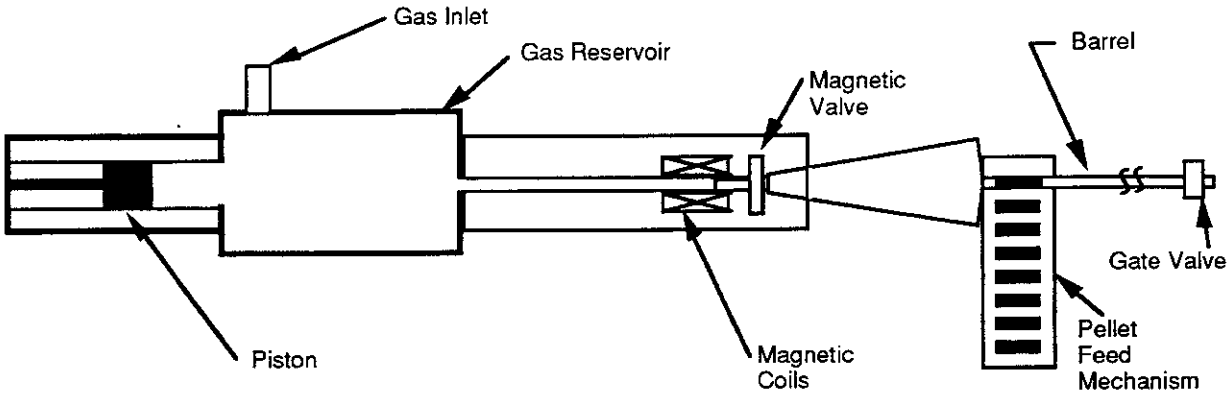

Figure 6.4.4-4. Constant Gas Pressure Is Maintained During Acceleration by a Piston in the Gas Reservoir.

References for 6.4

1. R. C. Davidson, et al., Inertial Confinement Fusion Reactor Design Studies Recommended Guidelines, Prepared for the Department of Energy, Office of Fusion Energy, September, 1990.

2. Roger O. Bangerter, "Revised Target Information for ICF Reactor Studies", 28 February 1991.

3. J. E. Howard, Appl. Opt., 16, p. 2764.

4. J. B. Trenholme and E. J. Goodwin, "Nova Target Illumination Studies," Laser Program Annual Report - 1980, LLNL Report UCRL-50021-80, Livermore, CA.

5. S. Skupsky and K. Lee, J. Appl. Phys., 54, p. 3662.

6. SOLASE - A Conceptual Laser Fusion Reactor Design, UWFDM-220, Section IX-B-1, December, 1977.

7. P. C. Souers, Hydrogen Properties for Fusion Energy, University of California Press, Los Angeles, 1986, pp. 85-87.

8. T.P. O'Holleran, R.L. Downs, D.A. Steinman and R.L. Crawley, *Journal of Vacuum Science and Technology*, 18 (3), pp. 1242-1243.

9. L. A. Scott, et. al., Journal of Vacuum Science and Technology A, 8 (3), pp. 1736-1740.

10. U. Kubo and H. Tsubakihara, Journal of Vacuum Science and Technology A, 5 (4), pp. 2778-80.

11. R. L. Downs, 1987 KMS Annual Report, p. 74.

12. L. A. Scott, et. al., op. cit.

13. H. W. Deckman, Journal of Vacuum Science and Technology, 18 (3), pp. 1171-1174.

14. J. K. Feuerherd and E. H. Farnum, Journal of Vacuum Science and Technology, 18 (3), pp. 1284-1287.

15. D. E. Day and C. P. Wang, Final Report to Los Alamos National Laboratory, Contract No. 9-X66-5788D-1, 1987

16. L. A. Scott, et. al., op. cit.

17. I. S. Goldstein, F. Falk and J. Trovato, Journal of Vacuum Science and Technology, 18 (3), pp. 1175-1178.

18. K. D. Wise, M. G. Robinson and W. J. Hillegas, Journal of Vacuum Science and Technology, 18 (3), pp. 1179-1182.

19. R. L. Downs, KMS Fusion, Inc. Annual Report, 1986, p. 90.

20. H. H. Johnson, Hydrogen in Metals, Proceedings of an international conference on the effects of hydrogen on materials properties and selection and structural design, pp. 35-49, 23-27 September, 1973.

21. A. R. Troiano, Hydrogen in Metals, Proceedings of an international conference on the effects of hydrogen on materials properties and selection and structural design, pp. 3-15, 23-27 September, 1973.

22. M. R. Louthan, Jr., Hydrogen in Metals, Proceedings of an international conference on the effects of hydrogen on materials properties and selection and structural design, pp. 53-77, 23-27 September, 1973.

23. M. O. Speidel, Hydrogen in Metals, Proceedings of an international conference on the effects of hydrogen on materials properties and selection and structural design, pp. 249-285, 23-27 September, 1973.

24. SOLASE, op. cit., p. IX-A-16.

25. R. L. Downs, op. cit., p. 89

26. A. J. Martin, KMS Fusion, Inc. Annual Report, 1986, p. 92.

27. KMS Fusion, Inc. Annual Report, 1985, pp. 99-102.

28. A. J. Martin, R. J. Simms, and R. B. Jacobs, Journal of Vacuum Science and Technology A, 6, p. 1885.

29. V. Varadarajan, K. Kim and T. P. Bernat, Journal of Vacuum Science and Technology A, 5 (4), pp. 2750-2754.

30. J. K. Hoffer and L. R. Foreman, Journal of Vacuum Science and Technology A, 7 (3), pp. 1161-1164.

31. A. J. Martin, KMS Fusion, Inc. Annual Report, 1988, pp. 13-17.

32. R. M. Singleton and J. T. Weir, Journal of Vacuum Science and Technology, 18 (3), p. 1264.

33. Hyo-gun Kim and M. D. Wittman, Journal of Vacuum Science and Technology A, 5 (4), pp. 2781-2784.

34. J. H. Pendergrass, D. B. Harris, and R. J. Dudziak, Fusion Technology, 13, pp. 375-395.

35. H. Sorenson, et. al., Proceedings of the 15th Symposium on Fusion Technology, Utrecht, The Netherlands, pp. 704-708, 19-23 September, 1988.

36. K. Sonnenberg, et. al., Proceedings of the 15th Symposium on Fusion Technology, Utrecht, The Netherlands, pp. 715-719, 19-23 September, 1988.

37. S. K. Combs, et. al., Journal of Vacuum Science and Technology A, 6 (3), pp. 1901-1904.

38. R. Kreutz, Fusion Technology, 8, pp. 2708-2720.

39. P. Michelson et. al., Proceedings of the 15th Symposium on Fusion Technology, Utrecht, The Netherlands, pp. 700-703, 19-23 September, 1988.

40. Y. C. Fung, Foundations of Solid Mechanics, Prentice-Hall, Inc., Englewood Cliffs, N. J., 1965, p. 191.

41. P. C. Souers, Hydrogen Properties for Fusion Energy, University of California Press, Los Angeles, p. 85, 1986.

42. K. Kawasaki, et. al., Proceedings of the 15th Symposium on Fusion Technology, Utrecht, The Netherlands, pp. 724-728, 19-23 September, 1988.

43. S. K. Combs, et. al., Proceedings of the 15th Symposium on Fusion Technology, Utrecht, The Netherlands, pp. 709-714, 19-23 September, 1988.

44. W. Bailey, et. al., Proceedings of the 15th Symposium on Fusion Technology, Utrecht, The Netherlands, pp. 720-723, 19-23 September, 1988.

45. H. Sorenson, et. al., op. cit.

46. K. Kawasaki, et. al., op. cit.

47. H. Hiratsuka et. al., Proceedings of the 15th Symposium on Fusion Technology, Utrecht, The Netherlands, pp. 729-732, 19-23 September, 1988.

48. K. Kawasaki, et. al., op. cit.

49. H. Sorenson, et. al., op. cit.

50. Ibid.